Journal of Visualized Experiments

Structural information from single-molecule FRET experiments using the Fast-Nano-Positioning System

--Manuscript Draft--

Manuscript Number:	JoVE54782R2
Full Title:	Structural information from single-molecule FRET experiments using the Fast-Nano-Positioning System
Article Type:	Invited Methods Article - JoVE Produced Video
Keywords:	Nano-Positioning System; Fast-NPS; single-molecule fluorescence; single-molecule Förster Resonance Energy Transfer; structural biology
Manuscript Classifications:	5.5.196.712.516.600.676.500: Fluorescence Resonance Energy Transfer (FRET); 8.1.671.100: Biophysics
Corresponding Author:	Jens Michaelis, Dr. Ulm University Ulm, Baden Württemberg GERMANY
Corresponding Author Secondary Information:	
Corresponding Author E-Mail:	jens.michaelis@uni-ulm.de
Corresponding Author's Institution:	Ulm University
Corresponding Author's Secondary Institution:	
First Author:	Thilo Dörfler
First Author Secondary Information:	
Other Authors:	Thilo Dörfler
	Tobias Eilert
	Carlheinz Röcker, Dr.
	Julia Nagy, Dr.
Order of Authors Secondary Information:	
Abstract:	Single-molecule Förster Resonance Energy Transfer (smFRET) can be used to obtain structural information on biomolecular complexes in real-time. Thereby, multiple smFRET measurements are used to localize an unknown dye position inside a protein complex by means of trilateration. In order to obtain quantitative information the Nano-Positioning System (NPS) uses probabilistic data analysis to combine structural information from X-ray crystallography with single-molecule fluorescence data to calculate not only the most probable position but the complete three-dimensional probability distribution, termed posterior, which indicates the experimental uncertainty. The concept was generalized for the analysis of smFRET networks containing numerous dye molecules. The latest version of NPS, Fast-NPS, features a new algorithm using Bayesian parameter estimation based on Markov Chain Monte Carlo sampling and parallel tempering that allows for the analysis of large smFRET networks in a comparably short time. Moreover, Fast-NPS allows to calculate the posterior by choosing one of five different models for each dye, that account for the different spatial and orientational behavior exhibited by the dye molecules due to their local environment. Here we present a detailed protocol for obtaining smFRET data and applying the Fast-NPS. We provide detailed instructions for the acquisition of the three input parameters of Fast-NPS: the smFRET values, as well as the quantum yield and anisotropy of the dye molecules. Recently, the NPS has been used to elucidate the architecture of an archaeal open promotor complex. This data is used to demonstrate the influence of the

	five different dye models on the posterior distribution.
Author Comments:	The first and the second author (Dörfler and Eilert) contributed equally to this work. Thus, both need to be indicated as first authors.
Additional Information:	
Question	**Response**
If this article needs to be "in-press" by a certain date to satisfy grant requirements, please indicate the date below and explain in your cover letter.	

TITLE:
Structural information from single-molecule FRET experiments using the Fast-Nano-Positioning System

AUTHORS:
Dörfler, Thilo †
Institute of Biophysics
Ulm University
Ulm, Germany
thilo.doerfler@uni-ulm.de

Eilert, Tobias†
Institute of Biophysics
Ulm University
Ulm, Germany
tobias.eilert@uni-ulm.de

Röcker, Carlheinz
Institute of Biophysics
Ulm University
Ulm, Germany
carlheinz.roecker@uni-ulm.de

Nagy, Julia
Institute of Biophysics
Ulm University
Ulm, Germany
julia.nagy@uni-ulm.de

Michaelis, Jens
Institute of Biophysics
Ulm University
Ulm, Germany
jens.michaelis@uni-ulm.de

† These authors contributed equally to this work.

CORRESPONDING AUTHOR:
Michaelis, Jens
jens.michaelis@uni-ulm.de

KEYWORDS:
Nano-Positioning System, Fast-NPS, single-molecule fluorescence, single-molecule Förster Resonance Energy Transfer, structural biology

SHORT ABSTRACT:
We present the setup and experimental procedure to obtain smFRET data from large donor-acceptor networks with a TIRF microscope. The step-by-step analysis of these measurements with the Bayesian inference software Fast-NPS yields high-resolved structural information via the application of adapted dye models.

LONG ABSTRACT:
Single-molecule Förster Resonance Energy Transfer (smFRET) can be used to obtain structural information on biomolecular complexes in real-time. Thereby, multiple smFRET measurements are used to localize an unknown dye position inside a protein complex by means of trilateration. In order to obtain quantitative information, the Nano-Positioning System (NPS) uses probabilistic data analysis to combine structural information from X-ray crystallography with single-molecule fluorescence data to calculate not only the most probable position but the complete three-dimensional probability distribution, termed posterior, which indicates the experimental uncertainty. The concept was generalized for the analysis of smFRET networks containing numerous dye molecules. The latest version of NPS, Fast-NPS, features a new algorithm using Bayesian parameter estimation based on Markov Chain Monte Carlo sampling and parallel tempering that allows for the analysis of large smFRET networks in a comparably short time. Moreover, Fast-NPS allows the calculation of the posterior by choosing one of five different models for each dye, that account for the different spatial and orientational behavior exhibited by the dye molecules due to their local environment.

Here we present a detailed protocol for obtaining smFRET data and applying the Fast-NPS. We provide detailed instructions for the acquisition of the three input parameters of Fast-NPS: the smFRET values, as well as the quantum yield and anisotropy of the dye molecules. Recently, the NPS has been used to elucidate the architecture of an archaeal open promotor complex. This data is used to demonstrate the influence of the five different dye models on the posterior distribution.

INTRODUCTION:
Determining the structure of a biomolecule is a key prerequisite for understanding its function. Two well-established methods for structure determination are cryo-electron microscopy and X-ray crystallography[1,2]. Today, both methods provide high-resolution structural information with a resolution down to the angstrom level. These two methods have been used extensively to elucidate the structure of large biomolecules such as protein complexes. Though the existing methods have constantly been improved throughout the last decades, the complexity of biological structures still poses a major challenge to structural biology, in particular when large, dynamic and transient complexes are investigated[3].

In order to study the dynamics of macromolecular complexes and the structure-function relationship in particular, single-molecule methodologies have provided useful[4]. Several new strategies were developed providing an orthogonal approach on acquiring structural and dynamic information. Examples are high speed AFM[5], mechanical manipulation[6], fluorescence

localization microscopy[7], as well as single-molecule Förster Resonance Energy Transfer (smFRET)[8,9]. Since quite early on FRET has been termed a *molecular ruler*, due to the distance dependence on the length scale of biomacromolecules[10].

One particularly interesting application of smFRET is to use the distance information obtained from smFRET measurements to infer structural information[11–23]. Due to the high time resolution of smFRET, the position of mobile parts of a protein structure can be localized. However, in order to extract quantitative information from smFRET data important correction parameters about the dye molecules need to be determined during the measurement[24]. With these correction factors, the FRET efficiency E_{FRET} can be calculated using the formula

$$E_{FRET} = \frac{I_A - \beta \cdot I_D}{I_A + \gamma \cdot I_D},$$

where I_A and I_D are the fluorescence intensities of the donor and the acceptor molecule, respectively (see Figure 2). The β-factor accounts for *cross-talk*, the leakage of donor emission into the acceptor channel and is calculated by

$$\beta = \frac{I'_A}{I'_D},$$

where I'_A and I'_D are the fluorescence intensities of the donor and the acceptor molecule after photo bleaching of the acceptor molecule.

The γ-factor corrects the difference in the relative detection efficiencies in the two channels as well as the differences in the fluorescence quantum yield of the donor and the acceptor dye. It is calculated from every individual time trace by

$$\gamma = \frac{\Delta I_A}{\Delta I_D} = \frac{I_A - I'_A}{I'_D - I_D}.$$

Note, that this description neglects direct excitation of the acceptor molecule, which sometimes becomes important and would need to be corrected for as well. For determining these correction factors it is useful to excite both the donor as well as the acceptor in an alternating scheme[25] in order to differentiate between photo-physical changes and structural dynamics.

In order to not only obtain quantitative smFRET efficiencies but also quantitative structural information, the Nano-Positioning System (NPS) was introduced in 2008[26]. The name was chosen based on its similarities to the satellite-based Global Positioning System (GPS). The NPS is a hybrid technique combining smFRET and X-ray crystallography data for the localization of unknown dye positions in biomacromolecular complexes. The crystal structure serves as a reference frame and the smFRET results are used to obtain distance information between an unknown fluorophore position (*antenna*) and a position known from the crystal structure (*satellite*). In consecutive

experiments the distances between the antenna and several satellites are measured and the position of the antenna is determined by means of a statistically rigorous analysis scheme based on Bayesian parameter estimation. As a result, not only the likeliest position of the antenna is computed, but its complete 3D uncertainty distribution, the so-called posterior, visualized by credible volumes. Moreover, NPS was expanded to allow for the analysis of complete smFRET networks[27].

The NPS has been used to solve a number of important questions in eukaryotic transcription, namely the course of the upstream DNA, the non-template DNA and the nascent mRNA within the RNA Polymerase II elongation complex[12,28], also demonstrating the effect of transcription initiation factors[26] and the dynamic architecture of an open-promotor complex[29]. Moreover, the NPS was used to elucidate the structure of the archaeal RNA Polymerase open complex[30] and in particular the position of transcription initiation factor TFE, which binds competitively to the same site as transcription elongation factor Spt4/5[31].

Since then, a number of smFRET based structural approaches have been published[15,18,21,23]. When comparing different smFRET based structural methods, it becomes clear that the apparent precision of the method is highly dependent on the particular choice of dye models. One should note that dye molecules may exhibit different spatial and orientational behavior depending on their local environment.

To this end, Fast-NPS was introduced[32]. Fast-NPS uses an advanced sampling algorithm reducing the calculation times drastically. Furthermore, Fast-NPS allows one to perform a structural analysis and for each dye molecule the user can choose from a set of five different dye models which will be described next. The most conservative model, called *classic*, assumes that the dye occupies only one, but unknown, position. At this position, the fluorophore can rotate freely within a cone, whose size is determined from its respective (time-dependent) fluorescence anisotropy. The orientation of the cone is not known, which leads to large uncertainties when converting measured smFRET efficiencies into distances. In this respect, the model is conservative, since it will lead to the smallest precision compared to the other dye models. Only for very short distances should the assumptions made by the classic model lead to a noticeably incorrect position determination. For typical smFRET values, the correct position is always enclosed in the comparatively large credible volume.

However, since a higher precision is desirable, it is important to develop and test alternative dye models, which could help to improve the precision. If the dye rotates much faster than its inherent fluorescence lifetime, the so-called *iso* model can be applied. Here, the orientation factor κ^2 (needed for calculating the characteristic isotropic Förster radius R_0^{iso}) is set to 2/3. As a result, the computed credible volumes are almost two orders of magnitude smaller as compared to those in the classic model[32]. In the case that the fluorophore is found in an environment that enables not only fast reorientation, but additionally fast motion all over its accessible volume, the *meanpos-iso* model should be used. In this model, the dye effectively occupies only one mean position, where the spatial averaging is accounted for by a polynomial distance conversion[15]. This model applies if for example the (commonly hydrophobic) dye is

attached to a hydrophilic region, e.g. the DNA. Application of the *meanpos-iso* model leads to a further reduction in the size of the credible volumes by a factor of approximately two. However, a dye linked to a protein might bind reversibly to several hydrophobic patches in its sterically accessible volume (AV). A fluorophore that instantaneously switches between these regions, but within one region undergoes free rotation and fast localized motion is best described by the *var-meanpos-iso* model. For a similar situation in which the dye is not free to rotate the *var-meanpos* model applies. More details about these models can be found in our recent publication [32].

These models provide an extensive repertoire to specifically account for the various environments a dye might encounter and applying them wisely optimizes its localization precision. In Fast-NPS every dye molecule attached to a specific position can be assigned to an individual model, such that FRET-partners are allowed to have different models. This enables limitless and close-to-nature modelling. However, it is important that one performs rigorous statistical tests to ensure that the result obtained by the final model combination is still in agreement with the experimental data. These tests are included in the Fast-NPS software.

In order to apply Fast-NPS to experimental data the measurement of (only) three input parameters is required. First, the dye-pair specific isotropic Förster radii (R_0^{iso}) have to be determined. Therefore, the quantum yield (QY) of the donor dye, the donor fluorescence emission spectra and the acceptor absorption spectra need to be measured. These measurements can be carried out in bulk, using a standard spectrometer and a standard fluorescence spectrometer. For each pair, the R_0 is then calculated using the freeware *Photochem CAD* and can be used in the NPS analysis. Moreover, the (time-resolved) fluorescence anisotropies of the dye molecules need to be obtained using a polarization (and time) sensitive fluorescence spectrometer. However, the most important input parameters for Fast-NPS are the smFRET efficiencies measured on a single-molecule fluorescence microscopy setup, such as a total internal reflection fluorescence microscope (TIRFM).

Here, we present a step-by-step protocol for obtaining smFRET data and applying Fast-NPS (Figure 1).

PROTOCOL:

1. Prerequisites and lab equipment

Note: The assembly of the measurement chamber is depicted in Figure 3. The sandwich-design of the measurement chamber comprises three major components: a quartz glass (fused silica) slide, a sealing film and a coverslip that seals the flow chamber. The measurement chamber is mounted onto a customized sample holder. The dimensions of the sample chamber and the metal holder are geared to fit to a standard microscopy quartz glass slide (76 x 26 mm).

1.1. Cut quartz glass slides using a diamond drill (0.75 mm) at positions indicated in Figure 4. The design of the quartz glass slides is asymmetric in order to differentiate between the two sides of each slide.

Note: The quartz slides can be re-used after the measurement until the surface becomes scratched.

1.2. To mount the chambers, use customized metal sample holders as depicted in Figure 5. The sample holders contain two threads (M4) in order to connect an inlet and an outlet tubing for the flow chamber. Furthermore, use threads (M3) to mount the sample chamber onto the metal holder as well as threads (M3) to fix the prism holder onto to the lower half of the metal holder.

1.3. Perform the smFRET measurements on a prism type total internal reflection fluorescence microscope (TIRFM) (Figure 6).

Note: The TIRFM features three lasers: A green (532 nm, Nd:YAG laser) and a red laser (643 nm, diode laser) for the excitation of the donor and the acceptor dye molecules as well as a blue laser (491 nm, diode-pumped solid-state laser) for bleaching the background fluorescent impurities on the sample chamber prior to the smFRET measurement. The three laser beams are spatially combined and can be selected via an acousto-optic tunable filter (AOTF). The fluorescence light is collected by a high aperture objective, split into a donor and an acceptor channel by using a dichroic mirror and projected onto two EM-CCD cameras. The sample chamber is attached to a micrometer stage allowing movement in x- and y-direction with two stepper motors. A third piezo motor is used together with an IR-laser and a position sensitive detector to build an auto-focus system to ensure optimal focus throughout the experiment.

1.3.1. Use alternating laser excitation (ALEX) when dynamics in the FRET time trajectories are observed[25]. Such dynamics can be caused by either conformational changes within the molecules or by fluctuations in acceptor brightness and acceptor blinking.

Note: ALEX allows for the discrimination between these two possible causes and prevents misinterpretation of dynamic FRET trajectories. However, for reasons of simplicity, the protocol part is restricted to the analysis of movies taken without ALEX.

Caution: Class 3B lasers are used in the single-molecule fluorescence setup. Ensure that adequate laser safety precautions, according to local government regulations, have been taken before the system is operated.

1.4. Perform the absorption measurement used for determining the quantum yield on a UV-VIS spectrometer (see Materials and Methods).

1.5. Perform the measurement of the donor fluorescence emission spectrum, the acceptor absorption spectrum and the fluorescence anisotropy on a fluorescence spectrometer (see Materials and Methods).

1.6. Prepare sample chambers according to published procedures[33]. Alternatively the procedure described in [[34]] can be used.

1.7. Label the investigated samples with a donor-acceptor dye molecule pair suited for smFRET and ensure that there is a biotin moiety for the immobilization on the surface of the sample chamber.

Note: In order to localize an unknown antenna dye position with the Fast-NPS software different sample constructs are needed. Every construct needs to have one label at the unknown antenna dye position and one label at a satellite position known from the crystal structure. At least three different constructs with dyes attached to the antenna position and three different satellite positions are required for accurate results. Measurements between antennas as well as between satellites are also useful to improve the accuracy, however, this requires exchange of dye molecules which needs to be correctly entered in the analysis.

2. Mounting of flow chambers in a custom holder

2.1. Pull silicone tubing (0.8 mm ID, 2.4 mm OD) into hollow tab screws (M4) and cut the tubing on both ends straight leaving an overhang of 1 cm on both sides by using a sharp razor blade. Adjust the overhang of the tubing to about 2 mm on one side of the tab screw.

2.2. Mount the flow chamber into the sample holder in a way that the holes in the quartz glass slide match the threads in the sample holder. Tighten inlet and outlet screws gently to ensure that the inlet and outlet of the sample chamber are still penetrable. Gently tighten the four screws of the acrylic glass holder to fix the position of the flow chamber.

2.3. Cut silicone tubing (0.58 mm ID, 0.96 mm OD) into 20 cm long pieces. Insert one of the pieces to the inlet and the outlet screw of the measurement chamber. Close the inlet and outlet tubing by using a clamp.

Note: The assembled sample chambers can be stored at room temperature for up to two weeks.

3. smFRET measurement on the TIRF microscope

3.1. Use a syringe to wash the sample chamber with 500 µL of PBS. Prevent air bubbles from entering the sample chamber at all times by creating a droplet at the end of the inlet tubing before changing to a different buffer solution.

3.2. Flush the sample chamber with 100 µL neutravidin (0.5 mg/mL in PBS) solution and incubate 15 minutes at room temperature.

3.3. Wash out the neutravidin solution with 500 µL of PBS.

3.4. Screw the metal holder for the prism onto the sample chamber.

3.5. Mount the sample chamber to the micrometer stage of the TIRF-microscope. Make sure to mount the sample chamber horizontally as straight as possible in front of the objective to

avoid defocusing during scanning process.

3.6. Start the software controlling the EM-CCD cameras and the software for controlling the piezo-motors of the stage.

3.7. Adjust the focus of the microscope objective by looking at the reflections of the IR laser.

3.8. Place the prism (PS991, n = 1.52) on top of the metal prism holder. Adjust the lateral position of the prism to make sure that the laser beams hit the prism then use an adhesive and incubate with UV light for 5 min.

Note: Mounted prism can be reused by cleaning.

3.9. In the camera control software click “Setup Acquisition” and define the following acquisition parameters: 100 ms integration time, 401 frames/movie (green camera), 400 frames/movie (red camera), electron multiplier gain 225, pre-amplifier gain 5x and readout rate 3 MHz at 14 bit.

3.10. Create a folder on the local hard drive for the measurement. Choose a desired name for the measurement files, e.g.: Year-Month-Day. In the software settings go to the “Auto-Save” rider, enable “Auto save” and choose file format *.sif for movie acquisition. Select the folder on the hard disk. Use the folder name as filestem.

3.11. Enable the “AutoIncrement” function (set start value to 1). Enable the attachment of an operator to the filename. Use “DON” and “ACC” for the donor and the acceptor channel, respectively. Choose “_” as separator.

3.12. In the camera control software click on “Video” to start the live image of the camera and bleach background fluorescence by scanning the sample chamber using maximum laser intensity of all three lasers (combined ≈3000 W/cm^2 for 10 s per field of view).

3.13. Switch off the blue laser. Decrease the intensity of the green laser to around 200 W/cm^2 and to around 40 mW/cm^2 for the red laser if alternating laser excitation (ALEX) is used.

3.14. Dilute the biotinylated fluorescent sample to a concentration of 50-100 pM. Load 100 µL of the solution. The sample is immobilized on the chamber surface upon binding.

Note: Make sure not to overload the chamber. Neighboring molecules must be separated from each other.

3.15. If necessary, load an additional 100 µL of a 2x more concentrated sample to the chamber.

3.16. Seal the inlet and outlet tubing of the measurement chamber using clamps after loading

is completed.

3.17. Switch off all lasers and use the piezo-motors to move the flow chamber two fields of view further.

3.18. In the camera control software click on “Take signal” to start movie recording and switch on the laser at the same time. Ensure that more than 80% of the molecules are bleached by the end of the movie by adjusting the laser power.

3.19. Repeat steps 3.17 and 3.18 for the whole prebleached sample chamber region.

4. Acquisition of the transformation map (“beadmap”)

4.1. Prepare a flow chamber as described in Sections 1.1, 1.2 and 2.

4.2. Use avidin-coated fluorescent multispectral beads which show fluorescence emission in the donor and the acceptor channel. Vortex the stock for 1 minute, then dilute 50 µL of the stock in 50 µL ddH_2O. Vortex again for 1 minute, sonicate 1-2 minutes, then vortex another 10 s.

4.3. Carry out steps described for smFRET measurements (Section 3.5-3.10).

4.4. Load 100 µL (1 chamber volume) of the 1:2 diluted fluorescent beads into the flow chamber. Wait 10 minutes for the fluorescent beads to bind to the surface.

4.5. Use the acquisition parameters in 3.9 but change movie length to 26 (green camera) and 25 (red camera) and the electron multiplier gain to 10.

4.6. Set the intensity of the green laser to a value of 20 W/cm^2.

4.7. Take one movie at a field of view with approximately 50-100 beads.

5. Processing and analysis of smFRET data

5.1. Use the custom written software SM FRET for the analysis of the beadmap (see Materials and Methods) and the acquired movies. Start the program viewPlot1.m.

5.2. Click on Analysis|Batch Analysis, uncheck the option “ALEX” if it has not been used. For best performance choose the threshold for peak finding “high”. Press “OK”.

5.3. Choose “NO” when asked if you have already analyzed a beadmap. Browse the folder containing the acquired beadmap and select the *.sif file (by double-clicking on it). In the next dialogue window press “OK”.

Note: If a beadmap has already analyzed in a previous measurement, choose “YES” here and select the saved beadmap by browsing to the correct folder and double clicking on the beadmap

*.map file. Continue with step 5.8.

5.4. Choose two single beads positioned in opposite corners of the field of view. The pixel intensities are colour-coded from dark blue (low intensity) to dark red (high intensity).

5.5. Click on the center of the first bead. If the center of the molecule can be located clearly by the color-coding, choose “YES” or else click “NO” and choose a different molecule pair.

5.6. Position the crosshair on the pixel showing the maximum intensity and press “KEEP”. Repeat the process with the second channel.

5.7. Click on the molecule in the opposite corner and repeat steps 5.5 and 5.6.

Note: The relative pixel shift of the two channels is displayed in the command window and the transformation map is automatically saved as *.map file into the folder containing the beadmap *.sif file.

5.8. To load the donor and acceptor movies (*.sif) for the “batch analysis”, browse to the folder, select all movies that shall be analyzed and click on “OK”. In the next dialogue window, press “OK”.

Note: The batch analysis is finished when the last lane displayed in the command window starts with “Finished analyzing…”. The detected molecules are displayed in a new window, which also indicates the relative shift of the donor and the acceptor channel determined from the transformation map.

5.9. To load the batched movie files click on File|Load. Uncheck the option “ALEX” if it has not been used. Set the smoothwidth to 10 and click “OK”. Choose the folder containing the *.ttr files and click on “select all” and “OK” in the next context menu.

5.10. If the displayed trace features the characteristic smFRET phases (Figure 2) press on the toggle button “Not selected” and first select the time point of the beginning of the FRET event by moving the line with the mouse cursor and clicking the left mouse button. Next select the time point of the bleaching of the donor molecule and finally the time point of the bleaching of the acceptor molecule.

5.11. In the next window the FRET efficiency is plotted in blue. To select the trace press the “Yes” button otherwise choose “No”. To re-access a time trace click the “Prev” button.

5.12. Repeat the procedure until the last molecule of the movie.

5.13. After analyzing the last molecule in a movie save the selected traces by clicking on “File|Save”. Save the selected traces in the same folder as the *.sif files.

5.14. Repeat steps 5.10-5.13 for all acquired movies.

5.15. Execute the program *combine_fret_results.m*. Select the folder containing the *.res files and all the *.FRETonly_trace files. Save the molecule-wise FRET and frame-wise FRET files as MW.dat and FRW.dat, respectively.

Note: The *.dat files are saved as ASCII files. The FRW.dat file contains six columns and one row for each FRET-frame. The sixth column contains the corrected frame-wise FRET efficiency. The MW.dat file contains 21 columns and one row per selected FRET molecule. The third column contains the molecule-wise FRET efficiency.

6. Displaying smFRET data in histograms

Note: In order to extract the mean smFRET efficiency of all recorded smFRET data the frame-wise data or the molecule-wise data are plotted in histograms and analyzed using Gaussian fits to (multiple) peaks. In the following, the protocol uses a commercial data analysis software (see Materials and Methods). However any other available software can be used instead.

6.1. Open a data analysis software (see Materials and Methods). Click on File|Import|multiple ASCII. Select the folder containing the FRW.dat file. Select the file and press “OK”. Accept the input option with “OK” without a change.

6.2. Select the third column C(Y) containing the corrected FRET efficiencies, right-click on the column and select Plot|Statistics|Histogram. In the histogram window double-click on the columns and deselect “automatic binning” and select a desired bin-size, e.g. 0.05. Also choose beginning and end values, e.g. -0.025 and 1.025.

6.3. Select the columns of the histogram by left-clicking on them. Then right-click and choose “go to Bin Worksheet”. Select the “Counts” column by left-clicking on it and then right-click and select Plot|Column/Bar/Pie|Column.

6.4. In the column bar plot go to Analysis|Fitting|Nonlinear curve fit|Open dialog. Choose “Gaussian” under Function then go to the “Parameter” rider. Deselect auto parameter initialization. Fix the offset value (y0) at 0. Click on “Fit”.

Note: The fit function as well as the fitting details are now displayed in the column plot. The “xc” value gives the center of the fit function, i.e. the mean FRET efficiency that serves as the input parameter for the NPS software.

7. Measurement of the quantum yield

7.1. Perform quantum yield determination with the relative method similar to the procedure described by Würth et al.[35], using Rhodamine 101 dissolved in ethanol (QY = 91.5%) as a standard.

7.2. Record absorption spectra at a UV-VIS spectrometer using an 80 µL volume in an

absorption cuvette of 1 cm path length. The absorbance at the wavelength which will be used for fluorescence excitation has to be ≤ 0.05.

7.3. Record emission spectra on a lamp-calibrated spectrometer operated in photon-counting mode. Perform the measurements with Glan-Thompson polarizers in the excitation (0°) and emission (54.7°) path (magic angle conditions) using a spectral bandwidth of about 5 nm and 2.5 nm for the excitation and emission monochromator, respectively. Measure samples after transferring them to a fluorescence cuvette with 3 mm path length taking care that the count rate does not exceed 10^6 s^{-1}.

7.3.1. Calculate quantum yield according to

$$\Phi = \frac{n^2}{n_{std}^2} \cdot \frac{\int f(\lambda) d\lambda}{\int f_{std}(\lambda) d\lambda} \cdot \frac{\left[1 - 10^{-A^{std}(\lambda_{ex})}\right]}{\left[1 - 10^{-A(\lambda_{ex})}\right]} \cdot \Phi_{std}$$

where n and n_{Std} are the refractive indices of the solvent of the sample and the standard, respectively. $f(\lambda)$ and $f_{Std}(\lambda)$ are the fluorescence intensities of the sample and the standard at the wavelength λ. $A(\lambda_{ex})$ and $A^{std}(\lambda_{ex})$ are the absorbance of the sample and reference at the excitation wavelength and Φ_{std} is the quantum yield of the standard.

8. Calculation of the isotropic Förster Radius (R_0^{iso})

8.1. Calculate the isotropic Förster radius from the emission spectrum of the donor molecule, the absorption spectrum of the acceptor molecule, the quantum yield of the donor and the refractive index of the medium. Use the freeware *PhotochemCAD* for the calculation of R_0^{iso}. However any other available software can be used instead[36].

9. Measurement of the Anisotropies

9.1. Determine steady-state fluorescence anisotropies from recordings of fluorescence spectra with various excitation/emission polarizer settings (V/V, V/H, H/V, H/H)[36].

9.2. Calculate the G-factor, which corrects for polarization artefacts of the instrument, for each wavelength from the ratio

$$G(\lambda) = \frac{I_{HV}(\lambda)}{I_{HH}(\lambda)}$$

and use it to calculate the anisotropy value for each wavelength:

$$r(\lambda) = \frac{I_{VV}(\lambda) - G(\lambda) \cdot I_{VH}(\lambda)}{I_{VV}(\lambda) + 2G(\lambda) \cdot I_{VH}(\lambda)}$$

where I_{xy} inidicates the intensity for excitation polarization *x* and emission polarization *y*.

9.3. Average the values across the emission spectral range to calculate the steady-state fluorescence anisotropy.

10. Installation of Fast-NPS software

10.1. Download UCSF Chimera from http://www.cgl.ucsf.edu/chimera and follow the installation guide.

10.2. Go to the website of the "Institute of Biophysics" at Ulm University: https://www.uni-ulm.de/en/nawi/institute-of-biophysics/software.html. Download the current version of Fast-NPS and extract it to a folder of choice. Open the subfolder "Redistributable" and install the Visual C++ Redistributable which is appropriate for the system.

11. Centering the pdb file

11.1. Open the pdb file(s) of interest in Chimera. Select all atoms of the macromolecular complex and calculate the coordinates of the centroid (Tools|Structure Analysis|Axes/Planes/Centroids|Define centroid…|Ok).

11.2. Open the Reply Log (Favorites|Reply Log) and the Transformation Tool (Tools|Movement|Transform Coordinates). Enter the coordinates of the centroid shown in the Reply Log into the textbox "Shift" of the Transform Coordinates window and change the sign of every coordinate. Press "Apply" and save the file with "Save PDB" (File|Save PDB).

12. Setting up the position priors

Note: All values are considered in angstrom.

12.1. Start the technical computing language and change the current folder to the local Fast-NPS folder. Enter in the command window: FastNPS.

12.2. Create a new jobfile in the Project Manager (Project|New).

12.3. Set up the position prior (Tools|Model dye prior).

12.4. In the panel "prior basics" define the spatial resolution of the position prior by entering its value (2 is recommended).

12.5. Exclude the interior of the macromolecule by activating the check box and clicking on the "load PDB" button. Select and load the centered pdb file as described in Section 11.

12.6. Specify the approximate diameter (13 Å is recommended, see discussion) of the dye by entering its value.

12.7. Enter a skeletonization distance, i.e. the distance the dye molecule may penetrate into the macromolecule (2 Å is recommended).

12.8. In the panel "maximum prior size" enter the minimal and maximal coordinates of the position prior (recommended: x in [-150,150], y in [-150,150] and z in [-150,150]).

12.9. When defining a satellite, activate the checkbox “attachment via flexible linker” in the panel “prior basics” and enter in the panel “linker” the coordinates of the atom (in the centered pdb file) at which the dye molecule is attached. Further, specify the length and the diameter of the linker by entering their values (13 Å and 4.5 Å are recommended, see discussion). In case of an antenna skip this point.

12.10. Press the button “calculate accessible volume”.

12.11. Save the position prior and optionally export it for visualization purposes in e.g. Chimera.

13. Defining the network geometry

13.1. Open the Define Measurement Window (Mode|Edit Geometry).

13.2. Create a new dye molecule by pressing the button “New” in the panel “Dyes”.

13.3. Set its fluorescence anisotropy (Section 9) by entering a value and select a dye model within the dropdown menu “Dye model”.

13.4. Press the button “Load”, select the corresponding position prior and check the activate check box of the dye. Repeat this procedure for all dyes, i.e. for all antennas as well as for all satellites.

13.5. After creating all dyes, define the measurements. Create a new measurement by clicking “New” in the panel “Measurements”.

13.6. Select its FRET partners in the dropdown menus “Dye1” and “Dye2” below.

13.7. Enter the smFRET efficiency with error and the isotropic Förster radius of this dye pair.

13.8. Finally, check the activate check box of the measurement. Repeat this procedure for all measurements.

Note: Oftentimes the network becomes increasingly complex, so that the user might get confused. In order to prevent mistakes, you can check the network visually by pressing the “Check Network” button. The figure displays the activated dyes and indicates measurements via lines interconnecting the FRET dyes.

14. Calculation

14.1. Open the Calculation Window (Mode|Calculation).

14.2. If every dye in the network has a specific model assigned, select “User defined” and start the calculation by pressing “Calculation”. If you want to have all dyes in the same model,

select one of the five models (classic, iso, meanpos-iso, var-meanpos-iso and var-meanpo) and continue.

Note: The command window will indicate the progress of the calculation. Fast-NPS will do so with a pop-up message, when the calculation has been completed.

15. Visualization of results

15.1. In order to export the credible volumes of the dyes, open the View Results Window (Model|View Results).

15.2. Export dye densities:

15.2.1. Export dyes singly or all simultaneously. In order to export a single dye select it in the panel "Displayed Dyes" and press "Export Density". Enter a resolution (2 is recommended) and choose a file type for exportation. On the right the density is previewed and some of its mathematical characteristics are shown.

15.2.2. In order to export all dyes simultaneously push "Batch Export".

15.3. Open the resulting density files in Chimera.

16. Consistency check of chosen model combination

16.1. Open the View Results Window (Model|View Results). If in the panel "Calculation Info" the text box "Consistency" displays a value lower than 90% the current model does not represent the measured smFRET efficiencies sufficiently and is thus inconsistent.

16.2. In case of inconsistency push the button "Detailed Consistency". Search for the measurements that have a value below 90%. If one or more dyes are predominantly involved in these measurements, their models are likely to cause the inconsistency. Consider different dye models for these dyes and rerun the Fast-NPS calculation.

REPRESENTATIVE RESULTS:

Transcription is the first step in gene expression in all organisms. In Archaea, transcription is carried out by a single RNA polymerase (RNAP). Compared to eukaryotes, the archaeal RNAP bears a striking structural resemblance to their eukaryotic counterparts while having a simpler transcriptional machinery. Thus, Archaea can be used as a model system to study eukaryotic transcription initiation by RNA Polymerase II (Pol II). Recently, the complete architecture of the archaeal RNA polymerase open complex has been determined from single-molecule FRET and NPS. The data from NPS analysis was used to build a model of the complete archaeal open promotor complex, which provides useful insights into the mechanism of transcription initiation.

To elucidate this structure, smFRET efficiencies were measured between unknown antenna dye molecules located within the open promotor complex and several known satellite dye molecules that were incorporated at five reference sites in the RNAP, whose positions are known from

crystallographic structures (pdb-ID: 2WAQ)[37]. The antenna dyes were attached to either one of different positions on the non-template DNA, TFB, TBP or TFE. The complete network used in this study consisted of more than 60 measured distances.

Figure 7 depicts the model of the complete archaeal open promotor complex built from the NPS analysis. It comprises the double stranded promotor DNA (light and dark blue), the RNA Polymerase (grey) and the transcription initiation factors TBP (purple), TFB (green) and TFE (yellow). The model is superimposed with the results from the NPS analysis, the credible volumes, which were calculated using the classic model (A), the iso model (B), the meanpos-iso model (C), the var-meanpos-iso model (D) and the var-meanpos model (E).

Figure 1: Workflow of the acquisition and processing of the parameters needed for the Fast-NPS calculation.

Figure 2: Exemplary fluorescence intensity time trace of a smFRET event.
The fluorescence intensities of the donor (green) and the acceptor molecule (red) showing the three characteristic phases, namely I: smFRET, II: donor fluorescence after acceptor photobleaching, III: background fluorescence after donor photobleaching.

Figure 3: Schematic illustration of the flow chamber for smFRET experiments.
The flow chamber is mounted onto a customized metal holder with acrylic glass holders. The sandwich-design of the flow chamber comprises a quartz glass (fused silica) slide with two holes for attaching inlet and outlet tubing, a sealing film and a coverslip that closes the flow chamber. The prism for TIRF illumination is mounted onto the lower half of the flow chamber. Hollow tab screws provide the inlet and outlets for the flow chamber.

Figure 4: Preparation of the quartz glass slide and the sealing film.
Mechanical drawing of the quartz glass slide indicating the positions of the holes (given in millimeters).

Figure 5: Mechanical drawing of the flow chamber.
The measures for the aluminum prism holder, acryl glass holders and aluminum mounting frame are given in millimeters.

Figure 6: Schematic illustration of the prism-type TIRF setup used for smFRET experiments.
Abbreviations for optical components: A, aperture; DM, dichroic mirror; F, emission filter; L, lens; M, mirror; O, objective; P, prism; PSD, position sensitive photo-diode; S, sample; PS, positioning stage; T, telescope.

Figure 7: Simulation results of the different model assumptions.
All pictures show the archaeal RNA polymerase (pdb-ID: 2WAQ, top view) together with the model for promoter DNA (tDNA and ntDNA in blue and cyan, respectively), TBP (purple), TFB (green) and TFE (yellow) in the archaeal open complex[30]. The credible volumes are superimposed for the NPS simulation results of (A) the classic model, (B) the iso model, (C) the

meanpos-iso model, (D) the var-meanpos-iso model and (E) the var-meanpos model. All volumes are shown at 68% credibility. The classic and the var-meanpos networks are consistent with the smFRET data. In contrast networks where for all dyes the iso, meanpos-iso or the var-meanpos-iso model is chosen are inconsistent with the measured data.

DISCUSSION:

We present the setup and experimental procedure to accurately determine FRET efficiencies between dyes attached via flexible linkers to biomacromolecules, i.e. nucleic acids and/or proteins.

In order to ensure precise smFRET measurements (Section 3), it is crucial to exclude air from the flow chamber at any time during the measurement. Furthermore, make sure to not overload the flow chamber with fluorophores. The fluorophores must be clearly separated to ensure correct analysis. As smFRET pairs, which do not show bleaching of the donor have to be excluded from the analysis, make sure that >80% of the molecules in the field of view are bleached at the end of the movie. To account for inhomogeneities in the sample the β-factor and the γ-factor, correcting the cross-talk and relative detection efficiencies of the donor and acceptor channel, respectively, are calculated for each FRET pair individually.

The camera settings (integration time, electron multiplier gain, pre-amplifier gain and readout rate described in Section 3.9) should be set to values giving the best tradeoff between signal to noise ratio, dynamic range and time-resolution. They need to be re-adjusted for different experiments or if different hardware is used. The numbers of frames need to be high enough to ensure that most of the donor molecules bleach within the observation time."

For the measurements on the fluorescence spectrometer (Sections 7 to 9) a good compromise between the signal intensity and the spectral resolution of the recorded data has to be found. To this end the slits in the excitation and emission pathway of the fluorescence spectrometer have to be adapted dependent on the instrument used and the sample concentration.

Moreover, we present the Fast-NPS analysis method to obtain structural information of transient or dynamic macromolecular complexes. NPS has been applied to reveal the path of the non-template DNA strand and the position of transcription initiation factors in the archaeal RNA polymerase open complex. Using the network of more than 60 different distance measurements, we showed that Fast-NPS, equipped with a newly implemented sampling engine[38], reduces the time needed for the analysis of this complex smFRET network by ≈2 orders of magnitude, as compared to the original global NPS method[27]. The algorithm's robustness is rooted in a Metropolis-within-Gibbs sampler combined with a parallel tempering scheme. Fast-NPS shows exact reproducibility of network results and is consistent with results published earlier[30].

Several different methods have been published aiming to infer structural information from smFRET measurements [11–18]. All of these approaches provide only one specific dye model. Thus, dyes, that do not fulfill the assumptions made by the respective model, cannot be used or lead to false structural information. Fast-NPS, on the contrary, allows to select for each dye molecule

a different model. This helps to account for different conformational behavior of both, the dye molecule itself, as well as the linker used for its attachment. The local molecular surroundings of the dye molecule, as well as its physical properties will determine which model is most appropriate.

For the analyzed smFRET network of the archaeal initiation complex, an isotropic assumption for all dye molecules leads to a drastic decrease in the size of the credible volumes as compared to the classic model. In combination with a dynamic position averaging for all dye molecules the median of all credible volume sizes (at 95%) reduces to less than 0.5 nm^3. However, these dye molecule posteriors are no longer consistent with their smFRET measurements, indicating that the assumptions made lead to false structural information. In contrast, the posteriors determined in the classic model are consistent with the determined smFRET efficiencies.

As the assumption of isotropic and/or dynamic position averaging for all dyes lead to inconsistencies, Fast-NPS enables dye molecule priors in which each dye can be assigned one of the five models. Each model uses the same accessible volume. The algorithm for the calculation of the dye AVs makes several assumptions. At first, the fluorophore's spatial shape is approximated by a sphere. Thus, a diameter taking into account the fluorophore's width, height and thickness should be used (Section 12). Further, the linker's shape is approximated by a flexible rod. The values presented in Section 12 were computed for the dye Alexa 647 attached via a 12-C linker. To date, it is not possible to accurately determine a priori which model is most suited, given an experimental geometry, and thus all models should be tested. In general one will choose the model which gives the smallest possible posterior size, while still being consistent with the data. To test whether a choice of models is consistent with the smFRET data, we calculate both the posterior and the likelihood. Consistency means that more than 90% of the samples collected from the posterior are within the 95% confidence interval of the likelihood.

While it is true that the lower the anisotropy, the smaller the distance uncertainty, in a smFRET network geometric arrangements of the dye molecules also have to be taken into account. Thus, while representing dye molecules with a low fluorescence anisotropy with an iso model is a typical first choice, the consistency test provides a more direct means for selecting the correct dye model. The optimal choice of dye models can lead to a drastic increase in localization precision and at the same time retain the network's consistency with its FRET data.

To summarize, Fast-NPS allows to gain structural and dynamic information of large macromolecular complexes. In contrast to common structural methods such as x-ray crystallography or cryo electron microscopy this allows for monitoring highly flexible or transient complexes, thus greatly widening our mechanistic understanding of complex biological processes.

ACKNOWLEDGMENTS:
The authors thank B. Gruchmann for the mechanical drawings of the flow chamber. Further, we want to express our gratitude to Max Beckers and Florian Drechsler for insightful comments and discussions regarding NPS and the underlying sampling engine.

DISCLOSURES:
The authors have nothing to disclose.

REFERENCES

1. Cheng, Y. Single-Particle Cryo-EM at Crystallographic Resolution. *Cell.* **161** (3), 450–457, doi:10.1016/j.cell.2015.03.049 (2015).
2. Garman, E. F. Developments in X-ray Crystallographic Structure Determination of Biological Macromolecules. *Science.* **343** (6175), 1102–1108, doi:10.1126/science.1247829 (2014).
3. Sali, A. *et al.* Outcome of the First wwPDB Hybrid/Integrative Methods Task Force Workshop. **23** (7), 1156–1167, doi:10.1016/j.str.2015.05.013 (2015).
4. Hopfner, K. P. & Michaelis, J. Mechanisms of nucleic acid translocases: lessons from structural biology and single-molecule biophysics. *Curr Opin Struct Biol.* **17** (1), 87–95, doi:10.1016/j.sbi.2006.11.003 (2007).
5. Ando, T., Uchihashi, T. & Kodera, N. High-speed AFM and applications to biomolecular systems. *Annu Rev Biophys.* **42** (March), 393–414, doi:10.1146/annurev-biophys-083012-130324 (2013).
6. Neuman, K. K. C. & Nagy, A. Single-molecule force spectroscopy: optical tweezers, magnetic tweezers and atomic force microscopy. *Nat Methods.* **5** (6), 491–505, doi:nmeth.1218 [pii]\n10.1038/nmeth.1218 (2008).
7. Yildiz, A., et al. Myosin V walks hand-over-hand: single fluorophore imaging with 1.5-nm localization. *Science.* **300** (5628), 2061–2065, doi:10.1126/science.1084398 (2003).
8. Joo, C., Balci, H., Ishitsuka, Y., Buranachai, C. & Ha, T. Advances in Single-Molecule Fluorescence Methods for Molecular Biology. *Annu Rev Biochem.* **77** (1), 51–76, doi:10.1146/annurev.biochem.77.070606.101543 (2008).
9. Hohlbein, J., Craggs, T. D. & Cordes, T. Alternating-laser excitation: single-molecule FRET and beyond. *Chem Soc Rev.* **43** (4), 1156–71, doi:10.1039/c3cs60233h (2014).
10. Stryer, L. & Haugland, R. P. Energy transfer: a spectroscopic ruler. *Proc Natl Acad Sci U S A.* **58** (2), 719–726, doi:10.1146/annurev.bi.47.070178.004131 (1967).
11. Rasnik, I., Myong, S., Cheng, W., Lohman, T. M. & Ha, T. DNA-binding Orientation and Domain Conformation of the E. coli Rep Helicase Monomer Bound to a Partial Duplex Junction: Single-molecule Studies of Fluorescently Labeled Enzymes. *J Mol Biol.* **336** (2), 395–408, doi:10.1016/j.jmb.2003.12.031 (2004).
12. Andrecka, J., et al. Single-molecule tracking of mRNA exiting from RNA polymerase II. *Proc Natl Acad Sci U S A.* **105** (1), 135–140, doi:10.1073/pnas.0703815105 (2008).
13. Schröder, G. F. & Grubmüller, H. FRETsg: Biomolecular structure model building from multiple FRET experiments. *Comput Phys Commun.* **158** (3), 150–157, doi:10.1016/j.cpc.2004.02.001 (2004).
14. Margittai, M. *et al.* Single-molecule fluorescence resonance energy transfer reveals a dynamic equilibrium between closed and open conformations of syntaxin 1. *Proc Natl Acad Sci U S A.* **100** (26), 15516–21, doi:10.1073/pnas.2331232100 (2003).
15. Kalinin, S. *et al.* A toolkit and benchmark study for FRET-restrained high-precision structural modeling. *Nat Methods.* **9** (12), 1218–1227, doi:10.1038/NMETH.2222 (2012).

16. Choi, J. *et al.* N6-methyladenosine in mRNA disrupts tRNA selection and translation-elongation dynamics. *Nat Struct Mol Biol.* **23** (August 2015), 110–115, doi:10.1038/nsmb.3148 (2016).
17. Svensson, B. *et al.* FRET-based trilateration of probes bound within functional ryanodine receptors. *Biophys J.* **107** (9), 2037–2048, doi:10.1016/j.bpj.2014.09.029 (2014).
18. Stephenson, J. D., Kenyon, J. C., Symmons, M. F. & Lever, A. M. L. Characterizing 3D RNA structure by single molecule FRET. *Methods.* (2016), 1–11, doi:10.1016/j.ymeth.2016.02.004 (2016).
19. Lee, N. K. *et al.* Accurate FRET measurements within single diffusing biomolecules using alternating-laser excitation. *Biophys J.* **88** (4), 2939–2953, doi:10.1529/biophysj.104.054114 (2005).
20. McCann, J. J., Choi, U. B., Zheng, L., Weninger, K. & Bowen, M. E. Optimizing methods to recover absolute FRET efficiency from immobilized single molecules. *Biophys J.* **99** (3), 961–970, doi:10.1016/j.bpj.2010.04.063 (2010).
21. Brunger, A. T., Strop, P., Vrljic, M., Chu, S. & Weninger, K. R. Three-dimensional molecular modeling with single molecule FRET. *J Struct Biol.* **173** (3), 497–505, doi:10.1016/j.jsb.2010.09.004 (2011).
22. Schuler, B. Single-molecule FRET of protein structure and dynamics - a primer. *J nanoboitechnology.* **11** (Suppl 1), 1–17, doi:10.1186/1477-3155-11-S1-S2 (2013).
23. Choi, U. B., et al. Single-molecule FRET-derived model of the synaptotagmin 1-SNARE fusion complex. *Nat Struct Mol Biol.* **17** (3), 318–324, doi:10.1038/nsmb.1763 (2010).
24. Dale, R. E., Eisinger, J. & Blumberg, W. E. The orientational freedom of molecular probes. The orientation factor in intramolecular energy transfer. *Biophys J.* **26** (2), 161–193, doi:10.1016/S0006-3495(79)85243-1 (1979).
25. Kapanidis, A. N., et al. Alternating-laser excitation of single molecules. *Acc Chem Res.* **38** (7), 523–533, doi:10.1021/ar0401348 (2005).
26. Muschielok, A., et al. A nano-positioning system for macromolecular structural analysis. *Nat Methods.* **5** (11), 965–971, doi:10.1038/nmeth.1259 (2008).
27. Muschielok, A. & Michaelis, J. Application of the nano-positioning system to the analysis of fluorescence resonance energy transfer networks. *J Phys Chem B.* **115** (41), 11927–37, doi:10.1021/jp2060377 (2011).
28. Andrecka, J. *et al.* Nano positioning system reveals the course of upstream and nontemplate DNA within the RNA polymerase ii elongation complex. *Nucleic Acids Res.* **37** (17), 5803–5809, doi:10.1093/nar/gkp601 (2009).
29. Treutlein, B. *et al.* Dynamic Architecture of a Minimal RNA Polymerase II Open Promoter Complex. *Mol Cell* **46** (2), 136–146, doi:10.1016/j.molcel.2012.02.008 (2012).
30. Nagy, J. *et al.* Complete architecture of the archaeal RNA polymerase open complex from single-molecule FRET and NPS. *Nat Commun.* **6**, 6161, doi:10.1038/ncomms7161 (2015).
31. Grohmann, D. *et al.* The Initiation Factor TFE and the Elongation Factor Spt4/5 Compete for the RNAP Clamp during Transcription Initiation and Elongation. *Mol Cell.* **43** (2), 263–274, doi:10.1016/j.molcel.2011.05.030 (2011).
32. Beckers, M., Drechsler, F., Eilert, T., Nagy, J. & Michaelis, J. Quantitative structural information from single-molecule FRET. *Faraday Discuss.* **184**, 117–129, doi:10.1039/C5FD00110B (2015).

33. Bennink, M. L., et al. Unfolding individual nucleosomes by stretching single chromatin fibers with optical tweezers. *Nat Struct Biol.* **8** (7), 606–610, doi:10.1038/89646 (2001).
34. Chandradoss, S. D., et al. Surface passivation for single-molecule protein studies. *J Vis Exp.* (86), 4–11, doi:10.3791/50549 (2014).
35. Würth, C., Grabolle, M., Pauli, J., Spieles, M. & Resch-Genger, U. Relative and absolute determination of fluorescence quantum yields of transparent samples. *Nat Protoc.* **8** (8), 1535–1550, doi:10.1038/nprot.2013.087 (2013).
36. Lakowicz, J. R. *Principles of Fluorescence Spectroscopy*. doi:10.1007/978-0-387-46312-4 (Springer US: Boston, MA, 2006).
37. Korkhin, Y. *et al.* Evolution of complex RNA polymerases: The complete archaeal RNA polymerase structure. *PLoS Biol.* **7** (5), doi:10.1371/journal.pbio.1000102 (2009).
38. Eilert, T., Beckers, M., Drechsler, F. & Michaelis, J. in preparation.

Figure 1

Click here to download Figure Fig 1.jpg

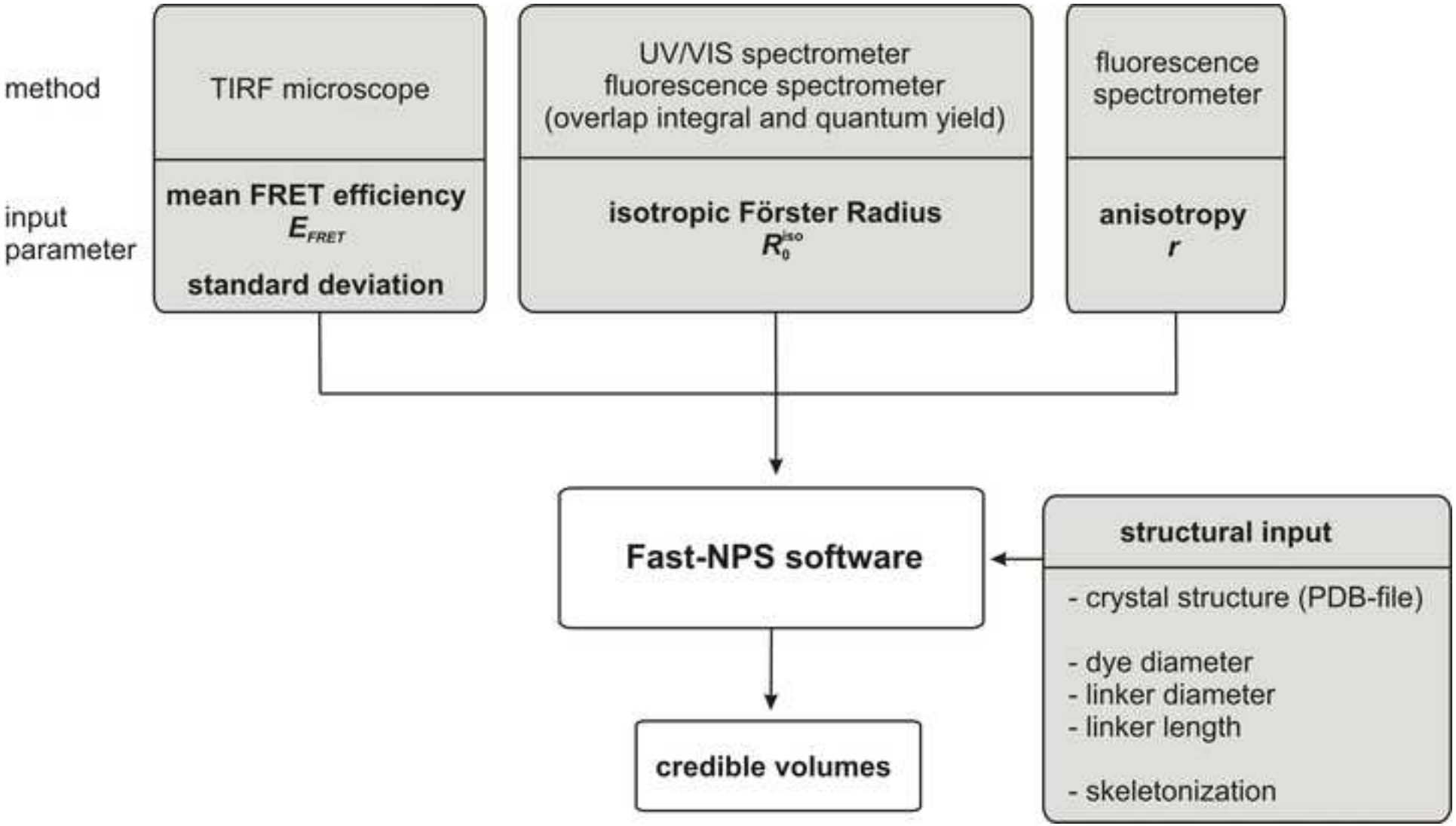

Figure 2

Click here to download Figure Fig 2.JPG

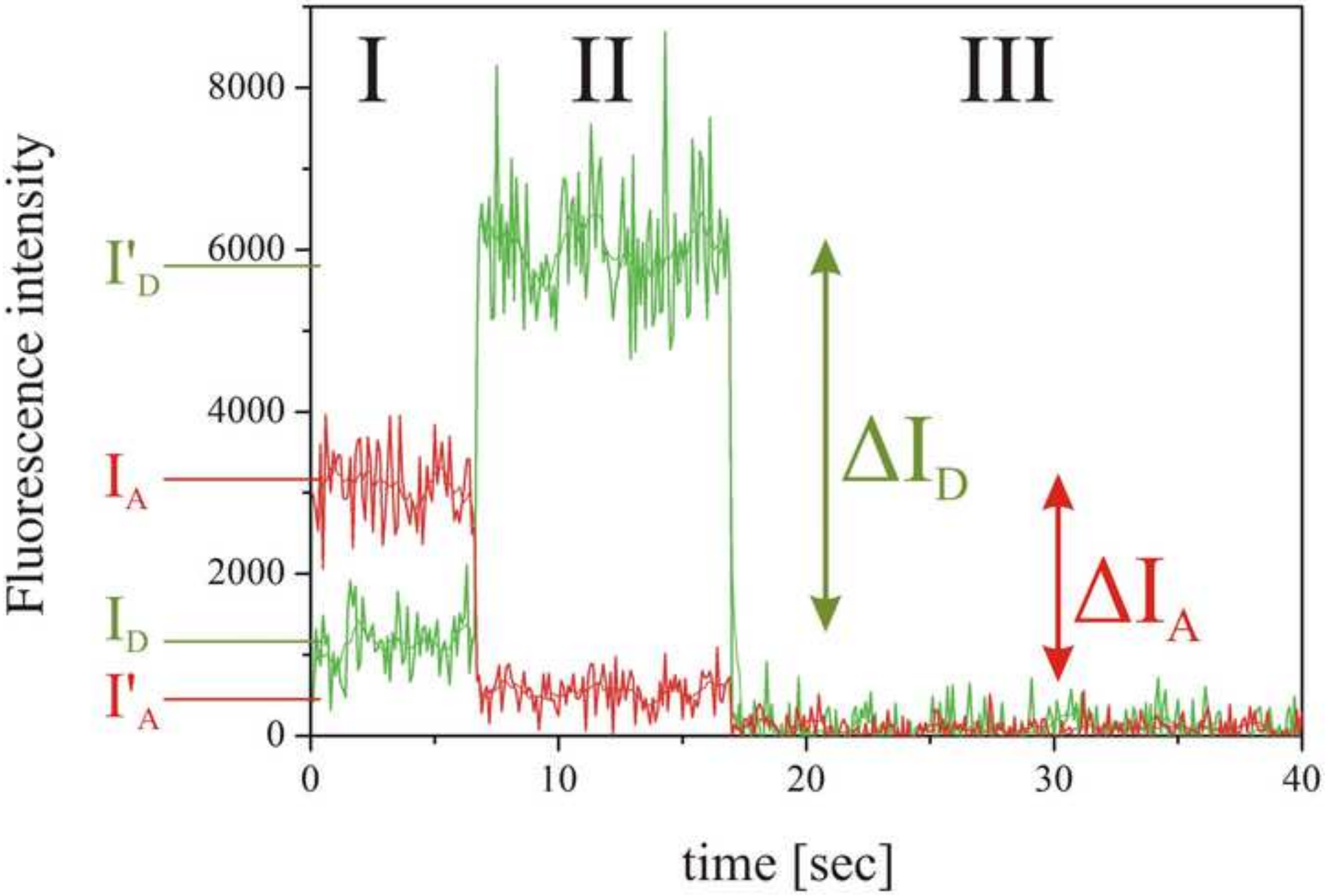

Figure 3

Click here to download Figure Fig 3.jpg

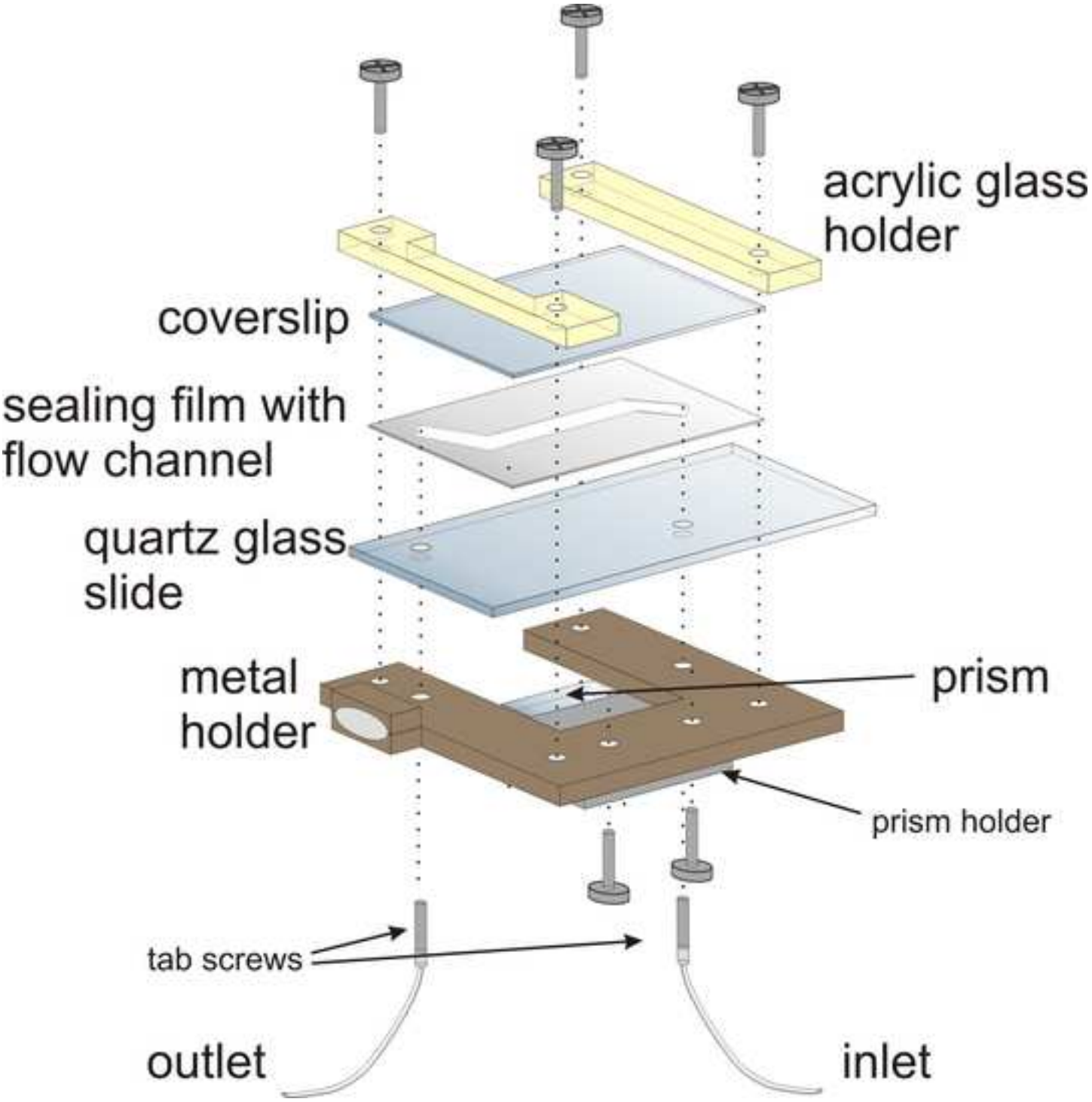

Figure 4

Click here to download Figure Fig 4.pdf

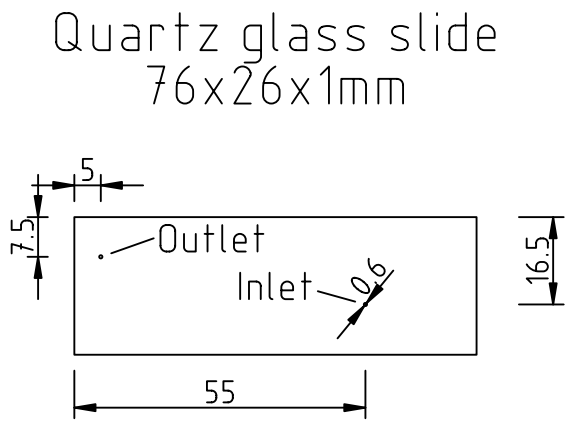

Figure 5

Click here to download Figure Fig 5.pdf

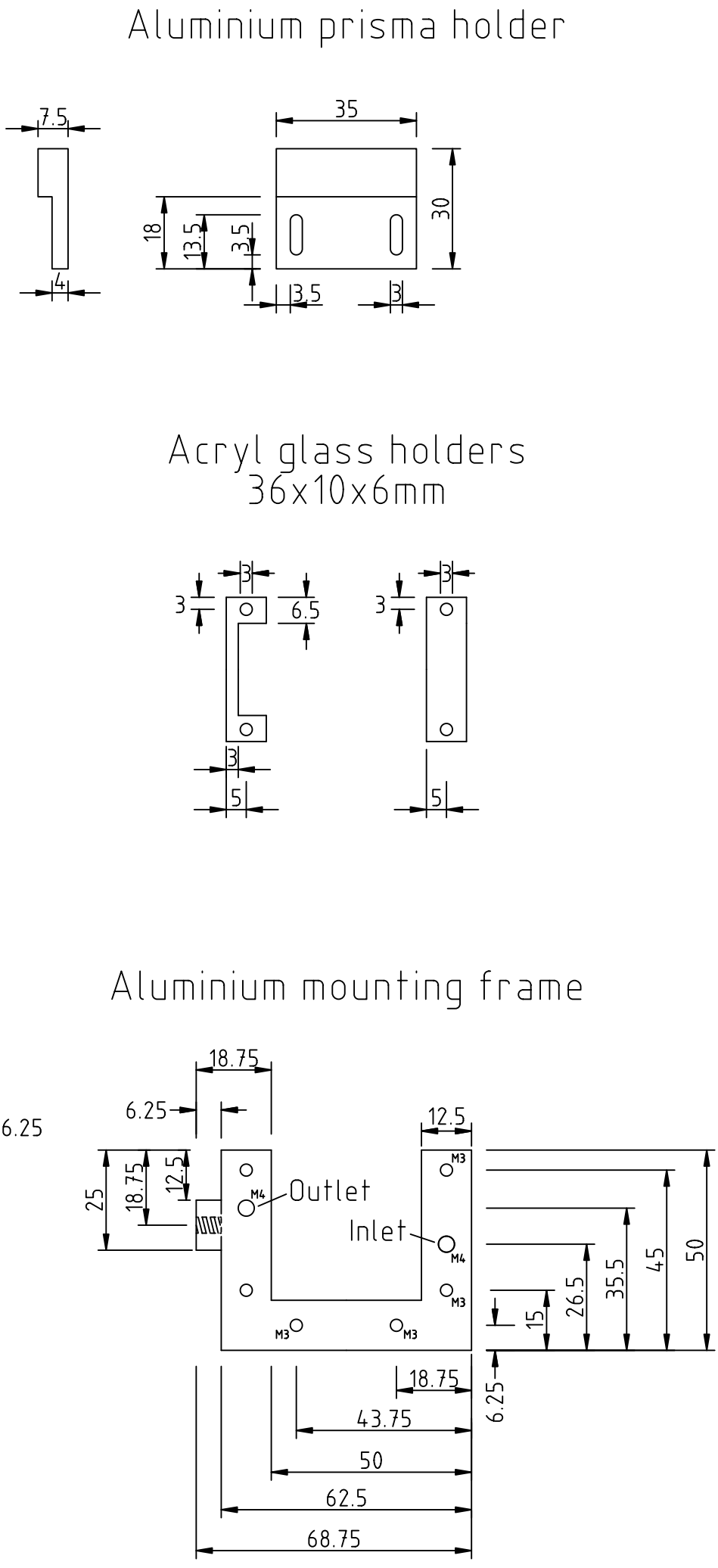

Figure 6

Click here to download Figure Fig 6.jpg

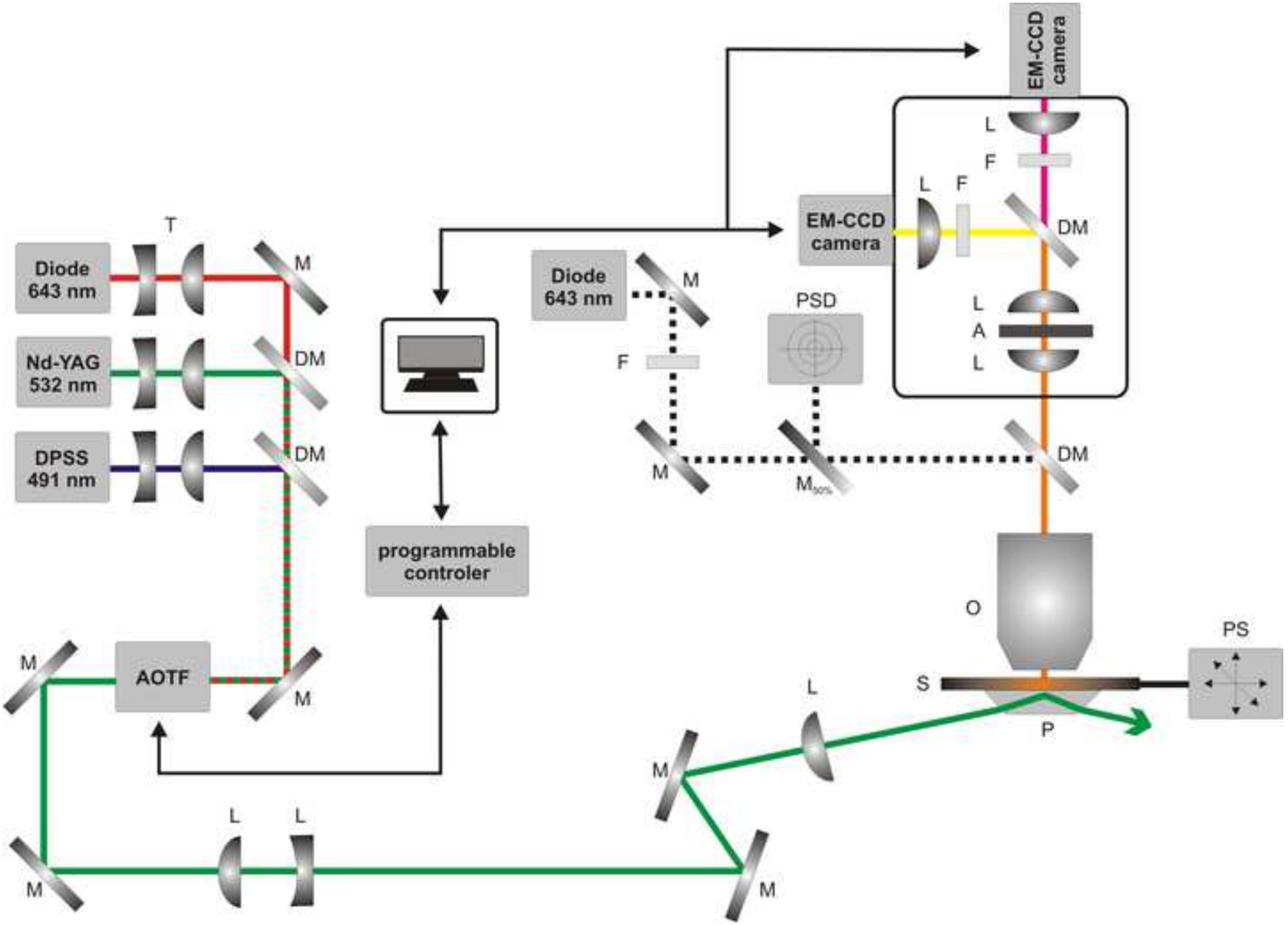

Figure 7

Click here to download Figure Fig 7.jpg

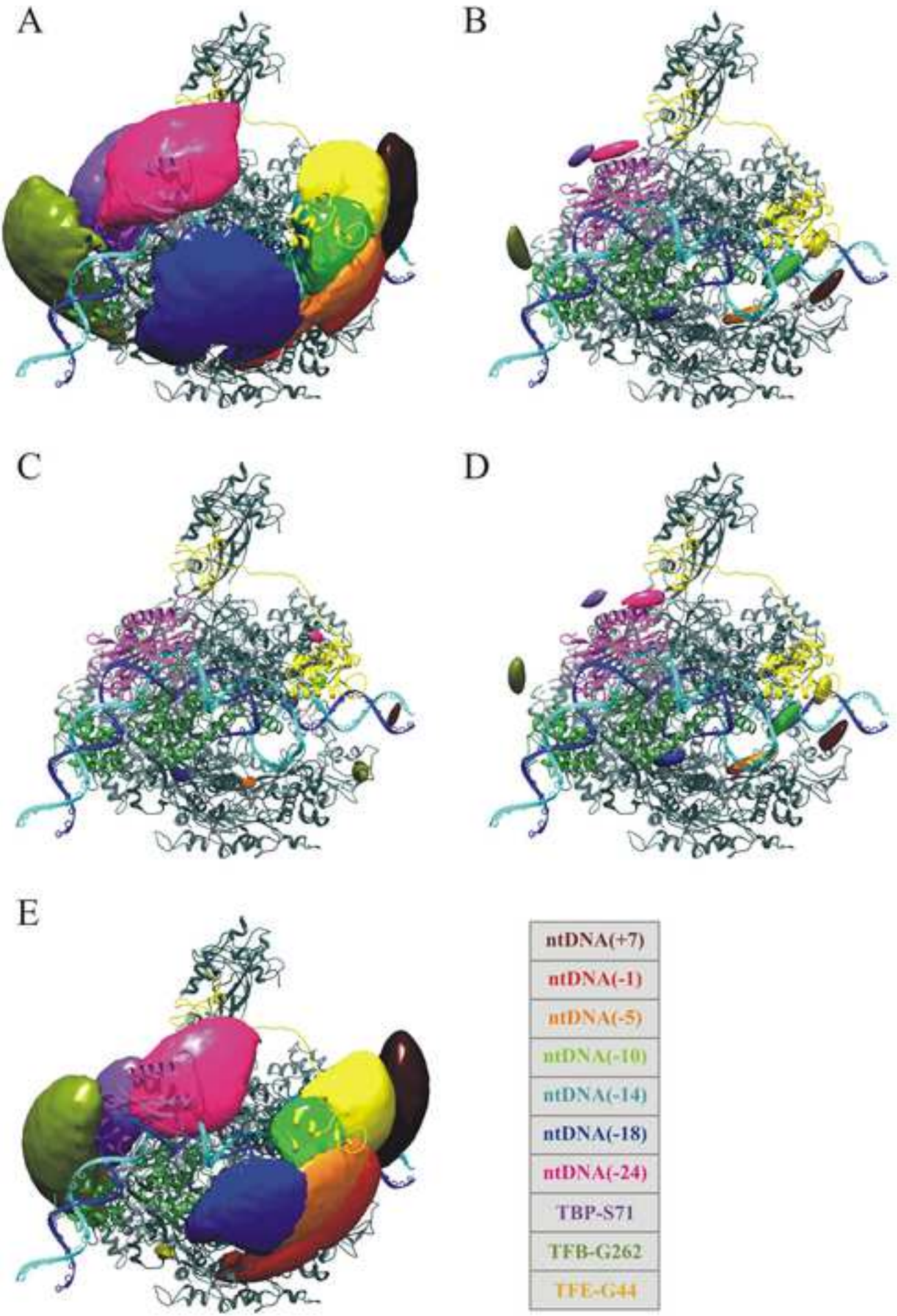

Excel Spreadsheet- Table of Materials/Equipment

Click here to download Excel Spreadsheet- Table of Materials/Equipment Materials and Equipment.xls

Name of Reagent/ Equipment	Company	Catalog Number	Comments/Description
Flowchamber preparation			
Customized metall sample holder	self-built	n/a	
quartz-glass slides, 76 x 26 mm	Technical Glass Products	26007	
coverslips, 60 x 24 mm	Marienfeld	101242	
detergent, Hellmanex II	Hellma	320.001	
ultra-pure water from Synergy UV	Millipore	2512600	
Zepto plasma cleaner	Diener	n/a	
(3-aminopropyl)-triethoxysilane, p.a.	Sigma-Aldrich	A3648	
methoxy PEG-succinimidyl valerate, 5 kDa	Laysan Bio Inc.	MPEG-SVA-5000-1g	
biotinylated PEG-succinimidyl valerate, 5 kDa	Laysan Bio Inc.	BIOTIN-PEG-SVA-5000	
Sodium biocarbonate	Sigma-Aldrich	S5761 Sigma	
Sodium carbonate	Sigma-Aldrich	S2127 Sigma-Aldrich	
sealing film (Nescofilm)	Fisher Scientific	12981805	
Tygon Flexible Silicone Tubing, 0.8 mm ID, 2.4 mm OD	Saint-Gobain Performance Plastics	720958	
Fine-Bore Polyethylene Tubing, 0.58 mm ID, 0.96 mm OD (Smiths Medical)	Fisher Scientific	12665497	
Neutravidin	Life Technologies	A2666	
Total internal reflection fluorescence microscope			
Nd:YAG Laser, 532 nm	Newport Spectra-Physics	EXLSR-532-100-CDRH	
diode-pumped solid-state laser, 491 nm, Calypso	Cobolt	904010050	
diode laser 643 nm, iBeam smart	Toptica	iBEAM-SMART-640-S	

dichroic mirror, 532 RDC	Chroma	F33-540	
dichroic mirror, 476 RDC	Chroma	F33-476z	
acousto-optic tunable filter	AA Opto-Electronic	AOTFnC-VIS	
plano-convex cylindrical lens, f = 75 mm	Thorlabs	LJ1703L1-A	
plano-concave cylindrical, f = -300 mm	Thorlabs		
prism, PS 991	Thorlabs	PS991	
focussing lens, f = 75 mm	Thorlabs	LA1608-B	
syringe pump, PHD 2000	Harvard Apparatus	70-2002	
2 stepper motors, Z812B	Thorlabs	Z812B	
piezoelectric actuator, PE4	Thorlabs	PE4	
IR diode laser	Edmund Optics	CPS808	part of the autofocus system
dichroic mirror, 775 DCXR	Chroma	775 DCXR	
position-sensing detector (PSD), PDP90A	Thorlabs	PDP90A	part of the autofocus system
water-immersion objective, Plan Apo 60X WI, NA 1.2	Nikon		MRD07601
dichroic mirror, 645 DCXR	Chroma	645 DCXR	part of the emission pathway
emission filter, 3RD550-510	Omega Optical	3RD550-510	green channel in the emission pathway
emission filter, 3RD660-760	Omega Optical	3RD660-760	red channel in the emission pathway
EMCCD camera, iXon+ DU897EBV	Andor	AND-20-00032	
EMCCD camera, iXon3 DU897D-BV	Andor	AND-20-000141	

Miscellaneous

Varian 50	Cary	UV-VIS spectrometer
Fluorolog2	SPEX	fluorescence spectrometer
Solis (V4.15)	Andor	control software for the EM-CCD camera
Apt user utility (V1.022)	Thorlabs	control software for the piezo-motors
Norland Optical Adhesive 68	Thorlabs	adhesive
PC-AFN-0.8 Nile red	Kisker Biotech	avidin-coated fluorescent multispec beads
Matlab	Mathworks	technical computing language for custon written soft
Origin (V9.0)	Originlab	scientific graphing and data analysis software

Hellma 105-202-15-40	Hellma	105-202-15-40	absorption cuvette of 1 cm path length
Hellma 105-251-15-40	Hellma	105-251-15-40	fluorescence cuvette with 3 mm path length

:ware

jove JOURNAL OF VISUALIZED EXPERIMENTS
1 Alewife Center #200
Cambridge, MA 02140
tel. 617.945.9051
www.jove.com

ARTICLE AND VIDEO LICENSE AGREEMENT

Title of Article: Structural information from single-molecule FRET experiments using the Fast-Nano-Positioning-System

Author(s): Dörfler, T.; Eilert, T.; Röcker, C.; Nagy, J.; Michaelis, J.

Item 1 (check one box): The Author elects to have the Materials be made available (as described at http://www.jove.com/publish) via: [X] Standard Access [ ] Open Access

Item 2 (check one box):

[X] The Author is NOT a United States government employee.

[ ] The Author is a United States government employee and the Materials were prepared in the course of his or her duties as a United States government employee.

[ ] The Author is a United States government employee but the Materials were NOT prepared in the course of his or her duties as a United States government employee.

ARTICLE AND VIDEO LICENSE AGREEMENT

1. Defined Terms. As used in this Article and Video License Agreement, the following terms shall have the following meanings: "**Agreement**" means this Article and Video License Agreement; "**Article**" means the article specified on the last page of this Agreement, including any associated materials such as texts, figures, tables, artwork, abstracts, or summaries contained therein; "**Author**" means the author who is a signatory to this Agreement; "**Collective Work**" means a work, such as a periodical issue, anthology or encyclopedia, in which the Materials in their entirety in unmodified form, along with a number of other contributions, constituting separate and independent works in themselves, are assembled into a collective whole; "**CRC License**" means the Creative Commons Attribution-Non Commercial-No Derivs 3.0 Unported Agreement, the terms and conditions of which can be found at: http://creativecommons.org/licenses/by-nc-nd/3.0/legalcode; "**Derivative Work**" means a work based upon the Materials or upon the Materials and other pre-existing works, such as a translation, musical arrangement, dramatization, fictionalization, motion picture version, sound recording, art reproduction, abridgment, condensation, or any other form in which the Materials may be recast, transformed, or adapted; "**Institution**" means the institution, listed on the last page of this Agreement, by which the Author was employed at the time of the creation of the Materials; "**JoVE**" means MyJove Corporation, a Massachusetts corporation and the publisher of *The Journal of Visualized Experiments;* "**Materials**" means the Article and / or the Video; "**Parties**" means the Author and JoVE; "**Video**" means any video(s) made by the Author, alone or in conjunction with any other parties, or by JoVE or its affiliates or agents, individually or in collaboration with the Author or any other parties, incorporating all or any portion of the Article, and in which the Author may or may not appear.

2. Background. The Author, who is the author of the Article, in order to ensure the dissemination and protection of the Article, desires to have the JoVE publish the Article and create and transmit videos based on the Article. In furtherance of such goals, the Parties desire to memorialize in this Agreement the respective rights of each Party in and to the Article and the Video.

3. Grant of Rights in Article. In consideration of JoVE agreeing to publish the Article, the Author hereby grants to JoVE, subject to **Sections 4** and **7** below, the exclusive, royalty-free, perpetual (for the full term of copyright in the Article, including any extensions thereto) license (a) to publish, reproduce, distribute, display and store the Article in all forms, formats and media whether now known or hereafter developed (including without limitation in print, digital and electronic form) throughout the world, (b) to translate the Article into other languages, create adaptations, summaries or extracts of the Article or other Derivative Works (including, without limitation, the Video) or Collective Works based on all or any portion of the Article and exercise all of the rights set forth in (a) above in such translations, adaptations, summaries, extracts, Derivative Works or Collective Works and (c) to license others to do any or all of the above. The foregoing rights may be exercised in all media and formats, whether now known or hereafter devised, and include the right to make such modifications as are technically necessary to exercise the rights in other media and formats. If the "Open Access" box has been checked in **Item 1** above, JoVE and the Author hereby grant to the public all such rights in the Article as provided in, but subject to all limitations and requirements set forth in, the CRC License.

4. Retention of Rights in Article. Notwithstanding the exclusive license granted to JoVE in **Section 3** above, the Author shall, with respect to the Article, retain the non-exclusive right to use all or part of the Article for the non-commercial purpose of giving lectures, presentations or teaching classes, and to post a copy of the Article on the Institution's website or the Author's personal website, in each case provided that a link to the Article on the JoVE website is provided and notice of JoVE's copyright in the Article is included. All non-copyright intellectual property rights in and to the Article, such as patent rights, shall remain with the Author.

5. Grant of Rights in Video – Standard Access. This **Section 5** applies if the "Standard Access" box has been checked in **Item 1** above or if no box has been checked in **Item 1** above. In consideration of JoVE agreeing to produce, display or otherwise assist with the Video, the Author hereby acknowledges and agrees that, Subject to **Section 7** below, JoVE is and shall be the sole and exclusive owner of all rights of any nature, including, without limitation, all copyrights, in and to the Video. To the extent that, by law, the Author is deemed, now or at any time in the future, to have any rights of any nature in or to the Video, the Author hereby disclaims all such rights and transfers all such rights to JoVE.

6. Grant of Rights in Video – Open Access. This **Section 6** applies only if the "Open Access" box has been checked in **Item 1** above. In consideration of JoVE agreeing to produce, display or otherwise assist with the Video, the Author hereby grants to JoVE, subject to **Section 7** below, the exclusive, royalty-free, perpetual (for the full term of copyright in the Article, including any extensions thereto) license (a) to publish, reproduce, distribute, display and store the Video in all forms, formats and media whether now known or hereafter developed (including without limitation in print, digital and electronic form) throughout the world, (b) to translate the Video into other languages, create adaptations, summaries or extracts of the Video or other Derivative Works or Collective Works based on all or any portion of the Video and exercise all of the rights set forth in (a) above in such translations, adaptations, summaries, extracts, Derivative Works or Collective Works and (c) to license others to do any or all of the above. The foregoing rights may be exercised in all media and formats, whether now known or hereafter devised, and include the right to make such modifications as are technically necessary to exercise the rights in other media and formats. For any Video to which this Section 6 is applicable, JoVE and the Author hereby grant to the public all such rights in the Video as provided in, but subject to all limitations and requirements set forth in, the CRC License.

7. Government Employees. If the Author is a United States government employee and the Article was prepared in the course of his or her duties as a United States government employee, as indicated in **Item 2** above, and any of the licenses or grants granted by the Author hereunder exceed the scope of the 17 U.S.C. 403, then the rights granted hereunder shall be limited to the maximum rights permitted under such statute. In such case, all provisions contained herein that are not in conflict with such statute shall remain in full force and effect, and all provisions contained herein that do so conflict shall be deemed to be amended so as to provide to JoVE the maximum rights permissible within such statute.

8. Likeness, Privacy, Personality. The Author hereby grants JoVE the right to use the Author's name, voice, likeness, picture, photograph, image, biography and performance in any way, commercial or otherwise, in connection with the Materials and the sale, promotion and distribution thereof. The Author hereby waives any and all rights he or she may have, relating to his or her appearance in the Video or otherwise relating to the Materials, under all applicable privacy, likeness, personality or similar laws.

9. Author Warranties. The Author represents and warrants that the Article is original, that it has not been published, that the copyright interest is owned by the Author (or, if more than one author is listed at the beginning of this Agreement, by such authors collectively) and has not been assigned, licensed, or otherwise transferred to any other party. The Author represents and warrants that the author(s) listed at the top of this Agreement are the only authors of the Materials. If more than one author is listed at the top of this Agreement and if any such author has not entered into a separate Article and Video License Agreement with JoVE relating to the Materials, the Author represents and warrants that the Author has been authorized by each of the other such authors to execute this Agreement on his or her behalf and to bind him or her with respect to the terms of this Agreement as if each of them had been a party hereto as an Author. The Author warrants that the use, reproduction, distribution, public or private performance or display, and/or modification of all or any portion of the Materials does not and will not violate, infringe and/or misappropriate the patent, trademark, intellectual property or other rights of any third party. The Author represents and warrants that it has and will continue to comply with all government, institutional and other regulations, including, without limitation all institutional, laboratory, hospital, ethical, human and animal treatment, privacy, and all other rules, regulations, laws, procedures or guidelines, applicable to the Materials, and that all research involving human and animal subjects has been approved by the Author's relevant institutional review board.

10. JoVE Discretion. If the Author requests the assistance of JoVE in producing the Video in the Author's facility, the Author shall ensure that the presence of JoVE employees, agents or independent contractors is in accordance with the relevant regulations of the Author's institution. If more than one author is listed at the beginning of this Agreement, JoVE may, in its sole discretion, elect not take any action with respect to the Article until such time as it has received complete, executed Article and Video License Agreements from each such author. JoVE reserves the right, in its absolute and sole discretion and without giving any reason therefore, to accept or decline any work submitted to JoVE. JoVE and its employees, agents and independent contractors shall have

jove
JOURNAL OF VISUALIZED EXPERIMENTS
1 Alewife Center #200
Cambridge, MA 02140
tel. 617.945.9051
www.jove.com

ARTICLE AND VIDEO LICENSE AGREEMENT

full, unfettered access to the facilities of the Author or of the Author's institution as necessary to make the Video, whether actually published or not. JoVE has sole discretion as to the method of making and publishing the Materials, including, without limitation, to all decisions regarding editing, lighting, filming, timing of publication, if any, length, quality, content and the like.

11. Indemnification. The Author agrees to indemnify JoVE and/or its successors and assigns from and against any and all claims, costs, and expenses, including attorney's fees, arising out of any breach of any warranty or other representations contained herein. The Author further agrees to indemnify and hold harmless JoVE from and against any and all claims, costs, and expenses, including attorney's fees, resulting from the breach by the Author of any representation or warranty contained herein or from allegations or instances of violation of intellectual property rights, damage to the Author's or the Author's institution's facilities, fraud, libel, defamation, research, equipment, experiments, property damage, personal injury, violations of institutional, laboratory, hospital, ethical, human and animal treatment, privacy or other rules, regulations, laws, procedures or guidelines, liabilities and other losses or damages related in any way to the submission of work to JoVE, making of videos by JoVE, or publication in *JoVE* or elsewhere by JoVE. The Author shall be responsible for, and shall hold JoVE harmless from, damages caused by lack of sterilization, lack of cleanliness or by contamination due to the making of a video by JoVE its employees, agents or independent contractors. All sterilization, cleanliness or decontamination procedures shall be solely the responsibility of the Author and shall be undertaken at the Author's expense. All indemnifications provided herein shall include JoVE's attorney's fees and costs related to said losses or damages. Such indemnification and holding harmless shall include such losses or damages incurred by, or in connection with, acts or omissions of JoVE, its employees, agents or independent contractors.

12. Fees. To cover the cost incurred for publication, JoVE must receive payment before production and publication the Materials. Payment is due in 21 days of invoice. Should the Materials not be published due to an editorial or production decision, these funds will be returned to the Author. Withdrawal by the Author of any submitted Materials after final peer review approval will result in a US$1,200 fee to cover pre-production expenses incurred by JoVE. If payment is not received by the completion of filming, production and publication of the Materials will be suspended until payment is received.

13. Transfer, Governing Law. This Agreement may be assigned by JoVE and shall inure to the benefits of any of JoVE's successors and assignees. This Agreement shall be governed and construed by the internal laws of the Commonwealth of Massachusetts without giving effect to any conflict of law provision thereunder. This Agreement may be executed in counterparts, each of which shall be deemed an original, but all of which together shall be deemed to me one and the same agreement. A signed copy of this Agreement delivered by facsimile, e-mail or other means of electronic transmission shall be deemed to have the same legal effect as delivery of an original signed copy of this Agreement.

A signed copy of this document must be sent with all new submissions. Only one Agreement required per submission.

CORRESPONDING AUTHOR:

Name: Jens Michaelis

Department: Institute of Biophysics

Institution: Ulm University

Article Title: Structural information from single-molecule FRET experiments using the Fast-Wand-Positioning-System

Signature: _____ Date: _____

Please submit a signed and dated copy of this license by one of the following three methods:

1) Upload a scanned copy of the document as a pfd on the JoVE submission site;
2) Fax the document to +1.866.381.2236;
3) Mail the document to JoVE / Attn: JoVE Editorial / 1 Alewife Center #200 / Cambridge, MA 02139

For questions, please email submissions@jove.com or call +1.617.945.9051

Response to Editorial and Reviewers' comments

Editorial comments:

Changes to be made by the Author(s):

1. Please take this opportunity to thoroughly proofread the manuscript to ensure that there are no spelling or grammar issues. The JoVE editor will not copy-edit your manuscript and any errors in the submitted revision may be present in the published version.

We have carefully checked the revised manuscript for errors.

2. Please upload the custom code files as Supplemental Code Files to be included with the manuscript upon publication.

The code files are yet unpublished and will be subject of an upcoming publication, where the latest software version will be made accessible. We are in the process of submitting that manuscript.

3. Formatting:
-3.9 and throughout the manuscript – Please use "sec" as the abbreviation for second(s).
-4.2 – "multispec" should be "multispectral"
-12.5 – Are you referring to "section 11"?

We have made these changes.

4. Grammar:
-Please use American English throughout. For instance, "polarisation" should be "polarization".
-4.11 – "choose "YES" else click "NO""
-5.7 – Please use imperative tense.
-"Tubing" should always be singular.

We have made these changes.

5. Visualization: Software usage must be performed in a GUI rather than entering commands into a terminal or running scripts. Please provide screenshots of the program used in sections 12 and 13 to confirm use of a GUI. If it is not a GUI, these sections cannot be filmed.

In the revised manuscript Section 12.1 is no longer highlighted. For the other sections we have added screenshots to ensure that these processes are performed in a GUI.

6. Additional detail is required:
-8.1, 9.1 – Please provide a citation.

We added the relevant citation.

-12.6 – What diameter is used here?
-12.9, 13.3 – What values are used here?

We added our recommended values to the corresponding sections in the protocol (see lines 569 and 581). The fluorescence anisotropy has to be measured by the researchers themselves according to Section 9, therefore we cannot give a specific value but included a cross reference to this section in line 594.

Furthermore, we included a paragraph in the discussion section with some general information about the calculation of the accessible volume (AV) of the dyes (lines 769 - 774)

"Each model uses the same accessible volume. The algorithm for the calculation of the dye AVs makes several assumptions. At first, the fluorophore's spatial shape is approximated by a sphere. Thus, a diameter taking into account the fluorophore's width, height and thickness should be used (Section 12). Further, the linker's shape is approximated by a flexible rod. The values presented in Section 12 were computed for the dye Alexa 647 attached via a 12-C linker."

-13.3 – What dye model is used here?

The user can decide which model is applied to which dye, i.e. he/she can choose between classic, iso, meanpos-iso, var-meanpos-iso and var-meanpos for every dye. Therefore, in the protocol we would rather not specify the choice as it is dependent on several parameters described in the introduction part. Please see also our reply to reviewer #3s comment 2.

-14.2 – What is meant by "one of the five models below"?

In the Calculation window the user can choose one of the five dye models described in the introduction: classic, iso, meanpos-iso, var-meanpos-iso and var-meanpos. By doing so, the individual selection of dye model combinations is overwritten and all dyes will be in the chosen model. If the user selects "User defined" the individual selection remains.

7. Branding should be removed from Figure 2 - Nesco

We have made the requested change.

Note: We added a new Figure, now Figure 1, according to one of reviewer #1s comments about the workflow. Therefore all the Figure numbering have changed in the new manuscript version.

Reviewers' comments:

Reviewer #1:
Manuscript Summary:
The submitted paper for JoVE provides a detailed instruction to determine accurate FRET values, related distances and meaningful location distribution of fluorescent dyes in biomolecules. The NPS of the Michaelis lab is one of the approaches following position triangulation to identify unknown dye positions and by this to determine structure (here in biomolecules). The group has made various contributions to the field of smFRET and in particular towards establishing smFRET as a quantitative ruler and tool for structural biology. The paper is well written, the content is sound and I have little requests for revisions. The paper details both the determination of all necessary correction factors, Förster radius and accurate FRET and provides sufficient advise to use custom-made software to reproduce the data presented here. The paper can be published without further review subject to minor changes:

-There are text parts highlighted in yellow; will this have any meaning later? Clarify

These highlighted parts are the essential protocol steps that will appear in the JOVE Video.

-Figure 1 looks like taken from a student practical (screenshot) and does not satisfy peer-review standards.

We have replaced Figure 1 with an appropriate figure.

-The paper (and its understanding) would benefit from a schematic figure showing the "workflow", i.e., where which data and parameters are processed

We agree with the reviewer, that a schematic Figure would be very helpful to understand the overall protocol. Therefore we added a Figure showing the workflow of the acquisition and processing of the parameters needed for the Fast-NPS calculation (new Figure 1).

-Maybe this is only a problem in the current version of the paper but the whole manuscript could be structured better to find e.g., a method better when mentioned somewhere in the text

In the discussion part we added cross references to the protocol sections to improve the structure of the manuscript. For example:

line 719: “In order to ensure precise smFRET measurements (Section 3), it is crucial…”
line 734: “For the measurements on the fluorescence spectrometer (Sections 7 to 9) a good compromise…”

-Please provide examples of data pieces of the whole procedure if the journal allows, i.e., quantum-yield determination (spectra etc.), how r0 is determined with spectra, QY etc., show the resulting FRET histogramme of the trace in Figure 1 etc. Since figure 4 shows only the final dye positions, I am always a fan of seeing the intermediate "results" in terms of numbers etc. also in the text (or in a table)

Due to space constraints we cannot give more details regarding those computations. However, one has to note that these procedures are standard and are performed routinely by many laboratories worldwide.

Reviewer #2:

Manuscript Summary:

Dörfler et al. present a method to obtain structural information from single-molecule FRET experiments. This is a very timely issue and the group of Jens Michaelis is one of the few leading groups in this field. The focus of the manuscript is on the description and use of a significantly improved version of their NPS-software, namely Fast-NPS. In my opinion the use of sophisticated software becomes more and more important and requires good guidelines and documentation. Therefore, I do support publication of this manuscript after the following issues are addressed:

1."Short Abstract" and line 681: Please omit "complete", because this manuscript does not provide enough information to build such a "complete setup", which likely is also not intended. Only building the flow-chamber is described in detail.

We corrected this in the revised manuscript.

2.Please review the literature in the introduction. This is too much self-focused.

We have carefully checked the introduction and have added several other references.

3.Third equation (line 115): Please give also the general definition of the gamma factor.

The general definition of the gamma factor is given in the sentence above the equation (lines 112). To clarify the connection between the definition and the given equation, we changed the sentence to:

"The γ-factor corrects the difference in the relative detection efficiencies in the two channels as well as the differences in the fluorescence quantum yield of the donor and the acceptor dye. It is calculated from every individual time trace by…"

4.Line 136: I do not understand this sentence

For a better understanding we modified the sentences (line 135) and moved it to a different position in the introduction to improve the flow (line 153).

"Fast-NPS uses an advanced sampling algorithm reducing the calculation times drastically. Furthermore, Fast-NPS allows to perform a structural analysis and for each dye molecule the user can choose from a set of five different dye models which will be described next."

5.Line 184: Lit. 29 is unpublished, which does not help at all, therefore please provide some more information, e.g. with the "representative result" (see below).

We agree with the reviewer that the unpublished literature is not a good reference here. The statistical tests we refer to are the consistency checks which are part of the JOVE protocol (section 16). We therefore included a clarifying sentence to line 191:

"These tests are included in the Fast-NPS software."

6.Line 209 and 216: I think that Fig. 3 and Fig. 4 are interchanged.

Indeed, these two figures were interchanged. We changed the order of these figures and the corresponding captions.

7.Line 286: Gravity will not help sedimentation at all in 15min, unless the chamber is mounted in a ultra-centrifuge…

We thank the reviewer for this comment and omitted the mention of gravity in the revised manuscript.

8.Line 396: Could you comment on the use of ALEX. Should ALEX not be used?

For simplicity we restricted the protocol part to the analysis of movies taken without ALEX. However, we added a note to the measurement prerequisites to explain the use of ALEX (section 1.3):

"Note: Alternating laser excitation (ALEX) can be used when dynamics in the FRET time trajectories are observed [Kapanidis et al., Acc Chem Res 38, 523 (2005)]. Such dynamics can be caused by either conformational changes within the molecules or by fluctuations in acceptor brightness and acceptor blinking. ALEX allows for the discrimination between these two possible causes and prevents misinterpretation of dynamic FRET trajectories. However, for reasons of simplicity, we restricted the protocol part to the analysis of movies taken without ALEX."

9.Line 479: Why are the slits set to these values? Are instruments with constant slits not usable?

We have changed the paragraph for clarification:

"7.3 Record emission spectra on a lamp-calibrated spectrometer operated in photon-counting mode. Perform the measurements with Glan-Thompson polarizers in the excitation (0°) and emission (54.7°) path (magic angle conditions) using a spectral bandwidth of about 5 nm and 2.5 nm for the excitation and emission monochromator, respectively."

Also we included a paragraph in the discussion section describing the general requirements for these values (line 734):

"For the measurements on the fluorescence spectrometer (Sections 7 to 9) a good compromise between the signal intensity and the spectral resolution of the recorded data has to be found. To this end the slits in the excitation and emission pathway of the fluorescence spectrometer have to be adapted dependent on the instrument used and the sample concentration."

10.Line 718: Please explain how "consistency with their smFRET measurements" is quantified. This is very important for choosing the dye model.

We have added a more in-depth discussion to the discussion section (line 777):

"To test whether a choice of models is consistent with the smFRET data, we calculate both the posterior and the likelihood. Consistency means that more than 90 % of the samples collected from the posterior are within the 95 % confidence interval of the likelihood."

11.Fig. 6: Please discuss the consistency with the smFRET measurements for the given structures.

We see that the suggested information is missing and would constitute an important feature in understanding the conclusion of this figure. Thus we added in line 710:

“The classic and the var-meanpos networks are consistent with the smFRET data. In contrast networks where for all dyes the iso, meanpos-iso or the var-meanpos-iso model is chosen are inconsistent with the measured data.”

Reviewer #3:

Manuscript Summary:

In the above article, the authors describe how to perform and analyze single-molecule FRET data (smFRET) for doing trilateration using their newly developed Fast Nano Positioning System software. The method is relevant and knowing how to apply this method could be very useful to various groups in the FRET community. Hence, publication of this article in the Journal of Visualized Experiments would be interesting. However, there are a couple of issues that should be addressed to reach the audience.

1) The authors describe 5 different potential models that can be used when determining absolute distances with smFRET data. A more thorough discussion of these models, a figure to help clarify the differences between the models, and a discussion regarding under what conditions which model is more appropriate would be helpful.

It is indeed a crucial prerequisite that one understands for which condition one needs to choose a specific model. Therefore, we explained in the introduction (line 153-183) which environments can lead to the different spatial and temporal behavior described by the dye models. For a more detailed description of the different models and their application the reader is advised to read the publication by Beckers et. al. [32]. To clarify this we have added the following sentence to the manuscript (line 183):

"More details about these models can be found in our recent publication [Beckers et al.]"

2) Related to the above point, very little is said regarding the anisotropy data. The authors should explain more what role anisotropy plays and what anisotropy values are consistent with which models.

The reviewer has pointed out one of the key aspects of the model selection. The fluorescence anisotropy may play an important role in the selection of the models. However, in our own experience we found that there is no one to one correspondence between anisotropy value and model selection. To address this point we have added the following statement to the discussion section (line 781):

"While it is true that the lower the anisotropy, the smaller the distance uncertainty, in a smFRET network geometric arrangements of the dye molecules also have to be taken into account. Thus, while representing dye molecules with a low fluorescence anisotropy with an iso model is a typical first choice, the consistency test provides a more direct means for selecting the correct dye model. The optimal choice of dye models can lead to …."

3) The protocol needs to be more generalized. My impression is that the protocol is useful for students in Ulm working on the exact instruments for which the paper was written. However, if I wish to reproduce these types of experiments in my own lab, there are many questions remaining. For example, when setting up the camera, very specific information is given (Lines 307-310). It would be helpful to know what the aim of using the given the settings is. If I have a different camera, I can then figure out what settings to use. After giving the general idea, listing the settings that authors use is great but not helpful in my own lab if I am not given more general information.

We are aware that there are many different camera types and microscope components available. However, we were following the JOVE guidelines by giving both, specific information and exact values for parameters used on our instruments in the protocol. To address the reviewer's point we have included a new paragraph to the discussion section (line 728):

"The camera settings (integration time, electron multiplier gain, pre-amplifier gain and readout rate described in Section 3.9) should be set to values giving the best tradeoff between signal to noise ratio, dynamic range and time-resolution. They need to be re-adjusted for different experiments or if different hardware is used. The numbers of frames need to be high enough to ensure that most of the donor molecules bleach within the observation time."

Also, the width of the slits used for the fluorescence spectroscopy measurements may depend on the spectrometer. More general information would be useful. These are only two examples of many.

Please see our reply to reviewer #2, comment 9 on the same concern.

At the end of section 4, the last instructions are to "Click "Cancel" in the next dialogue window". I am missing the bigger picture. What does "Cancel" do here? Normally, when I am finished with a task in a program, I do not press "Cancel"….

We agree with the reviewer that this last sentence is confusing. Therefore, we revised this part and clarified the working protocol by restructuring Sections 4 and 5. Section 4 now only describes the acquisition of the beadmap (Sections 4.1 to 4.7). Then Section 5 describes the protocol of processing the FRET data. We made some changes in the first steps of Section 5 which should now improve the understanding of this part.

4) What does the consistency check do? What is magic about 90?

See our reply to reviewer #2 above.

Specific Comments
5) Can the program handle site-specific quantum yields and thus Förster Radii?

The quantum yield of all the individual donors attached site specifically to the complex have to be measured one by one. This data is then used to calculate specific isotropic Förster Radii for every donor-acceptor pair. For further details please see sections 7 und 8. In the software one has to enter the specific isotropic Förster radius for each dye molecule.

6) Line 286: Remove the comment about gravity helping sedimentation. For a small protein, such as neutravidin, gravity plays no role.

We omitted the mention of gravity in the revised manuscript.

7) Line 396. 'uncheck the option "ALEX"'. Add something similar to line 411 ("when this option was not used during data collection")

This section was omitted for other clarifying reasons (see reviewer #3, comment 3).

8) Line 423. Should not this read "repeating 5.6?"

We modified the last sentence of section 5.11 (line 448) according to the editorial request to use the imperative tense, thereby omitting the reference to another section for simplification:

“To re-access a time trace click the “Prev” button.”

9) Line 688. : "As smFRET pairs, which do not show bleaching of the donor have to be excluded from the analysis…". This is not necessarily true. Please explain how to incorporate data when the donor bleaches before the acceptor. I realize it is suboptimal, but there are situations where it may be difficult to obtain molecules where the acceptor bleaches first.

The described protocol uses a molecule by molecule γ-correction for which it is required that i) the acceptor bleaches before the donor and ii) donor bleaching is observed. However, in a less stringent approach also a mean γ could be used. In this case these two steps are not necessary. This leads to a different analysis procedure which is beyond the scope of this paper.

10) Figure 1. Add lines to guide the eye.
We modified this Figure.

Picture of the GUI of the software